Transduction of skin-migrating dendritic cells by human adenovirus 5 occurs via an actin-dependent phagocytic pathway

Transduction of skin-migrating dendritic cells by human adenovirus 5 occurs via an actin-dependent phagocytic pathway.

AUTHORS:

Efrain Guzman[1]*, Geraldine Taylor[1], Jayne Hope[2], Rebecca Herbert[1], Carolina Cubillos-Zapata[1] and Bryan Charleston[1]

AFFILIATIONS:

[1] The Pirbright Institute. Ash Road, Woking, Surrey, GU24 0NF, United Kingdom

[2] The Roslin Institute University of Edinburgh, Easter Bush, Midlothian, EH259RG.

* Corresponding author: efrain.guzman@pirbright.ac.uk

RUNNING TITLE: Transduction of DC by AdV5

Subject Category: Animal DNA Viruses

Keywords: Dendritic cells, Adenovirus entry, Afferent lymph dendritic cells, Receptor-independent endocytosis

WORD COUNT:

Abstract: 229

Main Text: 6853

ABSTRACT

Dendritic cells (DC) are central to the initiation of immune responses and various approaches have been used to target vaccines to DC in order to improve immunogenicity. Cannulation of lymphatic vessels allows for the collection of DC that migrate from the skin. These migrating DC are involved in antigen uptake and presentation following vaccination. Human replication-deficient adenovirus (AdV) 5 is a promising vaccine vector for delivery of recombinant antigens. Although the mechanism of AdV attachment and penetration has been extensively studied in permissive cell lines, few studies have addressed the interaction of AdV with DC. In this study, we investigated the interaction of bovine skin-migrating DC and replication deficient AdV-based vaccine vectors. We found that despite lack of expression of CAR and other known adenovirus receptors, AdV readily enters skin-draining DC via actin-dependent endocytosis. Virus exit from endosomes was pH-independent and neutralizing antibodies did not prevent virus entry but did prevent virus translocation to the nucleus. We also show that combining adenovirus with adjuvant increases the absolute number of intracellular virus particles per DC but not the number of DC containing intracellular virus. This results in increased trans-gene expression and antigen presentation. We propose that in the absence of CAR and other known receptors, AdV5-based vectors enter skin-migrating DC using actin-dependent endocytosis which occurs in skin-migrating DC and its relevance to vaccination strategies and vaccine vector targeting is discussed.

INTRODUCTION

Vaccines based on replication incompetent adenovirus (AdV) vectors are safe and highly immunogenic, capable of inducing a full spectrum of adaptive humoral and cell-mediated immune responses, and of inducing protective immunity in a number of animal species including man (Dicks *et al.*, 2015; Green *et al.*, 2015; Taylor *et al.*, 2015).

Human adenovirus 5 (AdV5 and sometimes referred to as HAdV-C5), a species C adenovirus, is the most commonly studied adenovirus vector for both gene therapy and vaccination and so it is also the most studied in terms of cell entry, host responses and gene expression (Smith *et al.*, 2010). Epithelial cell models have been used to describe the mechanism of AdV5 entry and trafficking to the nuclear membrane (Svensson & Persson, 1984; Wolfrum & Greber, 2013). It is generally accepted that the first step in AdV5 entry to its target cell is the binding of the virus' fiber protein to CAR (Coxsackie B-Adenovirus Receptor), followed by the binding of the RGD motif on the penton base to cellular integrins ($\alpha_v\beta_3$ and $\alpha_v\beta_5$). This promotes virus endocytosis into clathrin-coated vesicles and triggers the first step of the uncoating program (Burckhardt *et al.*, 2011). Once inside the cell, the virus exits endosomal vesicles to the cytosol, where it utilizes microtubule motors to traffic to the nuclear membrane (Bremner *et al.*, 2009) and deliver its DNA through the nuclear pore (Puntener *et al.*, 2011).

Although CAR has been shown to be the primary receptor for AdV5 entry in epithelial cells, CAR is not expressed on all cells that can be infected with AdV5. For example, infection of Kupffer cells is mediated by human blood coagulation factor X binding to AdV5 hexon (Alba *et al.*, 2009; Kalyuzhniy *et al.*, 2008; Waddington *et al.*, 2008) and entry of AdV5 to human peripheral blood monocyte-derived dendritic cells involves CD209 (Adams *et al.*, 2009).

Since their identification (Steinman & Cohn, 1973), dendritic cells (DC) have become increasingly recognized for their crucial role as initiators and regulators of immune responses. Many studies of DC biology rely on the isolation of monocytes or macrophages from blood or tissues (such as spleen or bone marrow) (Rossi & Young, 2005; Steinman, 1991), followed by maturation with interleukin 4 (IL-4) and granulocyte-macrophage colony-stimulating factor (GM-CSF), or the harvesting of tissues followed by isolation of resident DC. The cannulation of lymphatic vessels provides *ex vivo* DC derived from relevant anatomical sites such as the skin that drain sites of vaccination (Hemati *et al.*, 2009; Hope *et al.*, 2006; Schwartz-Cornil *et al.*, 2006). Due to the complexity of the surgical procedure to cannulate lymphatic vessels, this is most easily performed in large animals, such as cattle and sheep. We and others have described afferent lymph dendritic cells (ALDC) as being FSC^{high} $MHCII^{+}$ $DEC\text{-}205^{+}$ $CD11c^{+}$ $CD8\alpha^{-}$ (Cubillos-Zapata *et al.*, 2011; Gliddon *et al.*, 2004; Hope *et al.*, 2006). Within this population, subpopulations of DC expressing various levels of SIRPα (CD172a), CD11a, CD26 and CD13 have also been described (Brooke *et al.*, 1998; Gliddon *et al.*, 2004; Gliddon & Howard, 2002; Howard *et al.*, 1997). Of these, the SIRPα^{+} DC population is targeted by various vaccine vectors and these cells are more efficient at antigen presentation compared to SIRP$\alpha^{neg/low}$ ALDC (Guzman *et al.*, 2012; Hope *et al.*, 2012).

In the current study, we describe the interaction between replication-deficient AdV5 with bovine ALDC that drain the skin. We show that macropinocytosis is the principal entry mechanism for AdV5 into ALDC and that the kinetics of virus internalization are much slower than previously described for epithelial cells. We also show that virus exit from endosomal compartments does not require an acidic microenvironment. Furthermore, neutralizing antibodies do not block internalization of AdV5 but prevent trans-gene expression. Finally, we demonstrate that emulsification of AdV5 in oil-in-water adjuvants

improve virus internalization into ALDC *in vitro*, increasing trans-gene expression and antigen presentation. Defining and manipulating entry pathways may enhance vaccine vector efficacy through improved antigen delivery and presentation.

RESULTS

Bovine afferent lymph DC are transduced by adenovirus-based vectors despite the absence of known adenovirus receptors.

We have previously shown that AdV5 injected subcutaneously or intramuscularly above the site of cannulation is internalized by migrating DC between 4 and 12 hrs post inoculation and that, *in vitro*, up to 40% of ALDC can be transduced by AdV5 using an moi of 100 (Cubillos-Zapata *et al.*, 2011). To define the mechanism by which AdV5 transduces ALDC (defined as FSC^{high} $MHCII^{+}$ DEC-205^{+} $CD11c^{+}$ $CD8\alpha^{-}$, Fig. 1a), we initially assessed the expression of CAR on bovine cells including ALDC. CAR was detected by Western blotting in enriched membrane fractions from 293 and bovine lung (BL) cells but not membranes from bovine ALDC, (Fig. 1b). We then used the virus overlay binding assay (VOPBA) to confirm binding of AdV5 to bovine CAR. Under denaturing and non-denaturing conditions, AdV5 bound to enriched membrane fractions from 293 and BL cells, but not from ALDC (Fig. 1c and 1d). To confirm that AdV5 was binding specifically to CAR, a rabbit polyclonal antibody raised against CAR was used to block binding of AdV5 to CAR in a competition VOPBA assay (Fig. 1e). These results indicate that although AdV5 can use CAR for binding to BL cells, CAR is not expressed on bovine ALDC and, therefore AdV5 utilises an alternative entry strategy for ALDC that is CAR-independent.

A number of different molecules have been implicated in AdV attachment to mononuclear phagocytic cells, including, MHC, CD80/86, CD209 and sialic acid (Chen & Lee, 2014). We used a combination of chymotrypsin, trypsin and papain to remove surface expression of known AdV receptors and brefeldin A to prevent their surface expression during transduction of ALDC. Following this treatment, the viability decreased to between 8 and 12% as measured by trypan blue exclusion (data not shown). MHC I (Fig. 2a), MHC II (Fig. 2b), CD80 (Fig. 2c), CD86 (Fig. 2d), and CD209, also known as DC-SIGN (Fig. 2e) were

completely removed by protease treatment and their reconstitution on the cell's surface prevented throughout the course of the experiments. Removal of sialic acid with neurominidase (Fig. 2f) was also complete. In all cases, these treatments did not result in a decrease transduction efficiency of ALDC by AdV5-GFP (Fig. 2g-l). Blocking the RGD-binding receptors with the antagonist Cyclo(Ala-Arg-Gly-Asp-3-Aminomethylbenzoyl decreased transduction efficiency of 293 cells but not ALDC (Fig. 2m and n). Finally, transduction of both 293 and ALDC was blocked by incubating in the presence of bovine hyperimmune serum against AdV5 (Fig. 2o and p). These results indicate that using the treatments indicated above, transduction of ALDC by AdV5 is not affected.

Transduction kinetics of ALDC.

To investigate transduction kinetics of ALDC by AdV5, we utilised biotinylated AdV5-GFP (moi = 100 vp/cell) to infect freshly isolated ALDC and 293 cells. After a 90 minute incubation at 4ºC or 37ºC, more than 60% of the biotinylated AdV5-GFP had attached to 293 cells (Fig. 3a). In contrast, less than 5% of the biotinylated AdV5-GFP had attached to ALDC at either temperature. We also blocked attachment of AdV5 to 293 cells at both temperatures using anti-CAR antibodies and, as expected, we were able to block 95-98% of the AdV5-bio signal (data not shown). To confirm that biotinylation of the virus did not interfere with its ability to transduce cells and express encoded proteins, we also measured GFP expression in these cells by flow cytometry (Fig. 3b). A 90 minute incubation of 293 cells with biotinylated AdV5 at +4ºC or 37ºC, followed by washing off the excess inoculum and subsequent overnight incubation, was sufficient to transduce more than 80% of the cells. In contrast, <1% of ALDC expressed GFP following the same protocol. To determine the minimum time required for transduction of cells by AdV5, 293 cells and ALDC were incubated with AdV5-GFP at 37ºC, the inoculum was washed off at one hour intervals, and the cells were incubated overnight. Transduction was measured by assessing the percentage of cells expressing GFP by flow cytometry. We determined that

1 hr incubation was sufficient for AdV5 to transduce and express GFP in 293 cells but that at least 5 hrs were required for ALDC to be significantly transduced by the virus (Fig. 3c). To determine the kinetics of transgene expression, ALDC cells were cultured with AdV5-GFP (moi = 100) at 37ºC without washing, and GFP expression was measured at various time points by flow cytometry (Fig. 3d). GFP-positive 293 cells were evident at 4 hrs post transduction and by 8 hrs most cells were expressing the transgene. In contrast, at least a 12 hr incubation period was required before a significant number of ALDC expressed GFP (Fig. 3d, $p = 0.0071$ %GFP expression in ALDC at 12 hrs compared to GFP expression at time 0). Expression of GFP in ALDC peaked after 24 hrs in culture. Interestingly, transgene expression in ALDC subsequently decreased and approached baseline levels by 48 hrs (Fig. 3d). These results indicate that the mechanism of AdV5 entry and trans-gene expression in ALDC is significantly different to that in CAR-expressing 293 cells.

ALDC actively uptake adenovirus.

We then analysed the ability of a number of endocytosis inhibitors to block AdV5 entry and subsequent transduction. A fluorometric assay based on the capacity of trypan blue to quench extracellular but not intracellular fluorescein (Wan *et al.*, 1993) was modified to determine the effect of various biochemical inhibitors on the capacity for ALDC to internalize fluorescein-labelled AdV5 (AdV5-Fluo). Incubation at 4ºC for 60 min followed by quenching with trypan blue blocked internalization of AdV5-Fluo and no fluorescence was detected in either cell type (Fig. 4b). All other treatments were carried out as described in Materials and Methods. In comparison with DMSO, treatment with the various inhibitors resulted in the following: treatment with filipin, which blocks caveolae and cholesterol-dependent endocytosis, and chlorpromazine (CPZ), which inhibits clathrin-dependent endocytosis, reduced AdV5-Fluo uptake by 293 cells, as expected, but not by ALDC. In contrast, treatment with cytochalasin D (CCD), which blocks actin polymerization and amiloride, which blocks Na^+ channels, both reduced the uptake of virus by ALDC (Fig. 4a

and b). Treatment with methyl-β-cyclodextrin (mβ-CD), which blocks cholesterol-dependent phagocytosis, did not have an effect on virus uptake in either cell type. Treatment with endocytosis inhibitors at the concentrations observed did not significantly increase the number of dead cells during the course of the assay (data not shown). This data indicates that actin polymerization and Na^+/H^+ exchange are required for AdV5 uptake by ALDC.

Transient association of AdV5 with early endosome markers.

Following clathrin-mediated endocytosis of AdV5 in 293 cells, virus can be detected within clathrin-coated vesicles (Ashbourne Excoffon *et al.*, 2003). These early endosomes are characterized by the presence of Rab5 and EEA1 (Christoforidis *et al.*, 1999). To determine if entry of AdV5 into ALDC was associated with early endosomes, purified ALDC were cultured with AF568-labelled AdV5 for 1 to 6 hrs and analysed by confocal microscopy. AdV5 could not be detected on the surface of ALDC until 3 hrs after addition of virus when it was found to be associated with dendrites or cell membranes (Fig. 5a). An hour later a greater number of virions were associated with the dendrites/cell membrane and virions were also observed within the cytoplasm (Fig. 5b). By 5 hrs post infection, a proportion of virions were localized in proximity to the nucleus (Fig. 5c). We then stained AdV5-infected ALDC with EEA1-specific antibodies to determine localization of AdV5 with early endosomes. Although co-localization of AdV5-AF568 with EEA1 was observed at 4 hrs post infection (Fig. 6a), co-localization events were rare, suggesting that virus exit from the phagosome/endosome occurs quickly after entry or that the majority of AdV are not associated with early endosomes. We then tracked the localization of AdV5-AF568 within ALDC using two different AF488-labelled tracers: dextran is used to track fluid-phase pinocytosis and albumin is known to enter cells using a mannose receptor-endocytosis pathway. We observed co-localization of AdV568 with dextran-AF488 but not with

196 albumin-AF488 (Fig. 6c-d), suggesting that AdV5 entry into ALDC is via fluid-phase
197 macropinocytosis.

198 **Exit of AdV5 into the cytosol of ALDC is not pH-mediated.**

199 Following uptake, a key step in AdV5 infection is the exit of virus or virus aggregates from
200 phagosomes/endosomes into the cytoplasm (Meier *et al.*, 2005). To define the
201 mechanisms associated with AdV5 exit in ALDC, cells were treated with inhibitors of the
202 intracellular acidic microenvironment such as bafilomycin, NH_4Cl or chloroquine, 60 min
203 prior to the addition of AdV5-GFP. Cells were then cultured for 4 hrs and GFP expression
204 measured by flow cytometry. None of the treatments significantly reduced the proportion of
205 ALDC or 293 cells expressing GFP (Fig. 7A). To confirm the presence of acidic
206 endosomes within ALDC, we utilized fluorescein-labelled dextran and fluorescein-labelled
207 AdV5. The fluorescence of fluorescein is optimal at pH7.5 and rapidly decreases in acidic
208 conditions. Under normal culture conditions, the fluorescence intensity (MFI) of
209 fluorescein-labelled dextran within ALDC decreases after a 4 hr incubation (Fig. 7b),
210 confirming the presence of dextran within endosomes and their subsequent acidification.
211 In contrast, fluorescein-labelled AdV5 within ALDC did not show a decrease in
212 fluorescence after a 4 hr incubation (Fig. 7b). As expected, normalization of intracellular
213 pH with 10 mM NH_4Cl, pH7.5, inhibited the reduction of fluorescence in dextran-loaded
214 ALDC. To confirm these results, we measured the relative fluorescence of fluorescein at
215 various pH and generated a standard curve (Fig. 7c). ALDC were incubated with
216 fluorescein-labelled AdV5 or dextran and fluorescence was measured by real time
217 fluorometry. Figure 7d shows that the fluorescence of dextran in ALDC decreases over
218 time as the fluorescein becomes protonated, but the fluorescence of AdV5 remains the
219 same suggesting that acidic endosomes are not involved in adenovirus uncoating in
220 ALDC.

Neutralizing antibodies do not prevent virus entry into ALDC.

An important hurdle to successful vaccination with viral vectors is the presence of neutralizing antibodies which can limit the efficacy of the vaccine. Most neutralizing antibodies are raised against the fibre protein of AdV and thus block virus attachment to its receptor (normally CAR). In light of our results, we sought to investigate the effect of neutralizing antibodies on AdV5 entry into ALDC. We incubated AdV5-568 with normal bovine sera, hyperimmune bovine sera to AdV5 or mouse monoclonal anti-hexon antibodies. Virus-Ab complexes were then added to cultures of ALDC and virus entry assessed by confocal microscopy, 4-6 hrs post infection. Interestingly, the mean number of intracellular AdV5 was significantly higher ($p=0.0027$) in the presence of bovine hyperimmune sera or mouse anti-hexon antibodies compared to normal bovine sera (S1a). However, even after 6 hrs in culture, virus complexed with antibody did not migrate to the nuclear membrane, but remained in the mid-cytoplasm (S1b) whereas AdV5, incubated with normal bovine sera, migrated and was located proximal to the nuclear membrane as expected (S1c). This data shows that the presence of neutralising antibodies does not prevent attachment of the virus to the cell but rather block a process downstream of virus penetration.

Oil-in-water adjuvants increase virus uptake and enhance antigen expression.

Various approaches have been proposed to improve targeting of AdV vectors to DC, including modification of the virus fibre protein to increase virus binding and penetration to DC. Previous observations by us and others (Cubillos-Zapata *et al.*, 2011; Ganne *et al.*, 1994) indicate that the use of oil-in-water emulsions as adjuvants to deliver AdV5-based vaccines significantly increases the magnitude of immune responses to the trans-gene *in vivo*. To identify the effect of adjuvanted vector on ALDC, AF568-labelled AdV5-GFP was prepared in an oil-in-water emulsion, or combined with the adjuvant without mixing, and incubated ALDC with the preparations. ALDC incubated with emulsified virus contained a

247 significantly greater number of intracellular virions compared to cells incubated with virus
248 in adjuvant without mixing or in PBS ($p = 0.0248$, Figures 8a, b and c). The mean
249 fluorescence intensity of GFP was greater (Fig. 8d) and expression was more sustained
250 (Fig. 8e) in ALDC incubated with emulsified virus than in cells incubated with the virus in
251 adjuvant without mixing or in PBS. However, the percentage of cells expressing the trans-
252 gene did not change (Fig. 8e). To confirm the effect of adjuvanted vector on antigen
253 presentation, AdV5 expressing mycobacterial antigen 85A (Ag85A, (Cubillos-Zapata *et al.*,
254 2011)) in adjuvant was prepared with or without mixing and incubated with ALDC. These
255 ALDC were then cultured with $CD4^+$ T cells obtained from MHC-matched, BCG-vaccinated
256 cattle. Ag85A-specific responses were significantly higher when AdV5-Ag85A was mixed
257 with adjuvant compared to AdV5-Ag85A without mixing or without adjuvant ($p = 0.0076$).
258 The number of IFN-γ producing cells was minimal when T cells were cultured with ALDC
259 exposed to AdV5-GFP with or without adjuvant, or to adjuvant alone (Fig. 8f). This data
260 shows that in the absence of genetic modification of the virus fibre, increased transduction
261 efficiencies can be achieved by the use of water-in-oil adjuvants.

262 **DISCUSSION**

263 We have previously shown that in contrast to monocyte-derived DC, ALDC can be readily
264 transduced by replication-deficient AdV5 (Cubillos-Zapata *et al.*, 2011), achieving up to
265 50% transduction of ALDC *in vitro* and up to 12% *in vivo*. ALDC can be separated into two
266 main subpopulations, $CD172\alpha^+$ and $CD172\alpha^-$; only the former can be transduced by AdV5
267 vectors both *in vitro* and *in vivo* (Cubillos-Zapata *et al.*, 2011). In the current study, we
268 aimed to characterize the mechanism of AdV5 uptake by ALDC further.
269 Since its discovery as a primary receptor for AdV5 (Bergelson *et al.*, 1997), it has been
270 widely accepted that CAR is involved in AdV5 attachment to target cells. However, a
271 number of other cell surface molecules, such as CD40, MHC II, CD46 and Fc receptors,

have been identified which appear to play an important role in AdV5 attachment (reviewed in (Zhang & Bergelson, 2005)). We could not prevent the transduction of ALDC by AdV5 following proteolytic cleavage of surface proteins or by using RGD-blocking peptides. Although there is evidence that DC-SIGN is involved in attachment of AdV5 to human monocyte-derived DC (Adams *et al.*, 2009), we could not replicate these results using bovine ALDC. This may be due to differences between the interaction of AdV5 between human and bovine DC or to differences between monocyte-derived DC and ALDC. Apart from an antibody against CD64 (FcγR), antibodies against bovine FcγR are not available, so it is possible for these receptors to be involved in AdV5 entry into bovine ALDC.

VOPBA has been used to identify the binding of dengue virus (Jindadamrongwech & Smith, 2004), pseudorabies virus (Karger & Mettenleiter, 1996) and respiratory syncytial virus (RSV) (Tayyari *et al.*, 2011) to cell receptors. We used this assay under denaturing and non-denaturing conditions to determine if a protein receptor for AdV5 on membrane-enriched fractions from ALDC could be identified. Although binding of virus to a protein present in enriched membrane fractions from 293 and BL cells could be detected, we could not identify binding of AdV5 to membrane proteins derived from ALDC (Figure 1). It is possible that our inability of identify an AdV5 receptor on ALDC is due to the stringency of the assay's conditions or the sensitivity of our assays. New technologies developed to identify protein-protein interaction, such as FRET or high affinity co-immunoprecipitation followed by highly sensitive mass spectrometry may help identify receptors involved in AdV attachment in the future.

Using biotinylated AdV5 we showed that the virus does not bind to the surface of ALDC as it does to the surface of 293 cells suggesting that internalization of AdV5 by bovine ALDC is mediated by CAR-independent macropinocytosis and similar pathways have been described for internalization other viruses such as influenza (de Vries *et al.*, 2011) and vaccinia (Sandgren *et al.*, 2010) by DC. Alternatively, it is possible for AdV5 to use low-

affinity receptors present on the surface of ALDC as observed in other systems, such as CD46 (Sirena *et al.*, 2004), αMβ2 and αLβ2 (Huang *et al.*, 1996) integrins. It is possible that labelling the virus with sulfo-NHS conjugates (biotin, AF569, fluorescein) changes the way the virus enters the cells. We have tried to address this possibility by using non-labelled virus as control and GFP as readout of transduction when at all possible.

Professional phagocytic cells such as DC have the capacity to take up small and large particles using a variety of mechanisms such as macro- and micropinocytosis (Platt *et al.*, 2010; Savina & Amigorena, 2007). Using biochemical inhibitors of endocytosis, we found that cytochalasin D (CCD) was able to block AdV5 uptake indicating that AdV5 internalization by ALDC is an actin-mediated process (Cooper, 1987), and that skin-migrating DC utilize their capacity as professional phagocytic cells to survey peripheral sites acquiring foreign antigens such as vaccine vectors, and processing these antigens prior to and on arrival to local draining lymph nodes. Interestingly, dynasore had no effect on endocytosis of AdV5 indicating that this process is clathrin-independent (Chen *et al.*, 2009) and therefore does not require the binding of RGD to cellular integrins. This suggestion is supported by the finding that RGD blocking peptides did not inhibit AdV5 internalization by bovine ALDC (Figure 2).

We then looked at events following virus internalization, and using confocal microscopy we observed occasional co-localization of AdV5 particles with the early endosome marker EEA1, but not with the late endosome marker LAMP1 (data not shown), supporting previous evidence of AdV5 exit from early endosomes to the cytosol (Svensson & Persson, 1984). Although it has been previously proposed that AdV5 exits early endosomal compartments following intra-endosome acidification (Greber *et al.*, 1993) and reviewed in (Smith *et al.*, 2010), we could not block virus transduction of ALDC using a number of lysosomotropic agents. Additionally, the fluorescence intensity of AdV5-fluorescein remained constant in ALDC over time whereas the fluorescence intensity of

fluorescein-labelled dextran declined as fluorescein became protonated (Figure 7b and d). Our data indicates that acidification of endosomes is not required for transduction of ALDC by AdV5 and this has been shown to be the case in other systems (Otero & Carrasco, 1987; Rodriguez & Everitt, 1996; Svensson & Persson, 1984), and although Suomalainen *et al*. found in epithelial cells that virus penetration is independent of low endosomal pH, it could still be inhibited by ammonium chloride; so it is possible that AdV5 exit to the cytosol requires acidification of endosomes in some cells but not others. This raises the question of how AdV5 exits endosomal compartments in ALDC. It has been proposed that viral (Suomalainen *et al.*, 2013) or cellular proteases degrade early endosomes (Wiethoff *et al.*, 2005) or perhaps a yet unknown mechanism is involved in this process and requires further investigation.

The presence of naturally-acquired neutralizing antibodies against AdV5 is one of the major obstacles in the deployment of effective recombinant AdV5 vaccine vectors (Ahi *et al.*, 2011). Antibodies bound to neutralizing epitopes on the virus surface normally prevent virus binding to the cell's receptors (Roy *et al.*, 2005; Sumida *et al.*, 2005). However, we observed that AdV hyperimmune bovine sera enhanced the uptake of AdV5 by ALDC, perhaps through the use of Fc receptors while blocking trans-gene expression. We could not test the effect of blocking Fc receptors due to the lack of available reagents to use in bovine cells. In the presence of AdV5-specific antibody, the AF568-labelled virions were not translocated to the nuclear membrane, but remained in the cytoplasm and the signal was eventually lost (data not shown). A similar phenomenon has been described previously in HeLa cells (Smith *et al.*, 2008), in which TRIM21 binds to antibody-AdV5 complexes and targets the complexes for proteasomal degradation (Mallery *et al.*, 2010). The role of TRIM21 in AdV5 degradation remains to be investigated in DC.

Various approaches have been proposed to improve targeting of AdV vectors to DC, including modification of the virus fibre protein to increase virus binding and penetration to

DC. In light of our current results and previous studies that have shown that AdV5 emulsified in an oil-in-water adjuvant and injected over the site of cannulation provides longer trans-gene expression and improved immunogenicity compared to non-adjuvanted virus (Cubillos-Zapata *et al.*, 2011), we sought to understand the mechanism of improved immunogenicity in the absence of clear virus fibre-receptor interactions. Cells transduced with adjuvanted virus contained more intracellular virions and trans-gene expression was stronger and longer-lasting than in cells transduced with virus in the presence of adjuvant but without emulsification, or in PBS. In presentation assays, antigen-specific IFN-γ T cell responses were higher when adjuvanted virus was used. This suggests that the oil-in-water emulsion provides a biological medium which is used by the DC to take up larger amounts of solute, in this case AdV5. This in turn translates into greater numbers of intracellular virions that have the capacity to translocate to the nucleus more effectively and for longer periods of time, or that the virions may be protected from intracellular degradation for a longer period of time when taken up in an adjuvant emulsion. This results in stronger trans-gene expression and thus antigen presentation. In addition, the adjuvant emulsion may activate TLRs which provide signals for the DC to be more effective at activating T cells. However, our controls suggest that this may not be the case since *in vitro* responses to AdV5-Ag85 in PBS are not significantly higher than responses to AdV5-Ag85 in adjuvant but without mixing (Figure 8f). Further studies are required to understand the relationship between biochemical adjuvants and DC. Ultimately, genetic modification of fibre protein will only be useful if a clear cellular receptor is identified in the target cell, therefore alternative approaches, such as oil-in-water emulsions, may be the most appropriate to improve AdV-based gene delivery.

In conclusion, here we describe the interaction of a replication-deficient AdV vector with skin-migrating bovine DC, which are collected by cannulation of lymphatic vessels and are

not subject to culture in laboratory conditions. We present evidence of the phagocytic action of these DC. Upon encountering virus, ALDC actively phagocytose the virus particles, perhaps using an unknown low-affinity receptor, and which takes between 3 and 4 hrs before virus particles can be observed intracellularly. Following entry, the virus quickly exits endosomal compartments via an unknown mechanism or is never associated with acidic endosomes, travelling to the nuclear membrane and so initiating trans-gene transcription and translation. Neutralizing antibodies do not only prevent virus entry into DC but enhance it whilst inhibiting translocation to the nucleus. Our data will be useful in understanding DC-vaccine interactions and will help further development and improvement of viral vectors. Defining and manipulating entry pathways may enhance vaccine vector efficacy through improved antigen presentation.

METHODS

Pseudoafferent lymphatic cannulation

MHC-defined (Ellis *et al.*, 1996; Ellis *et al.*, 1998), conventionally reared, 6 month-old Friesian Holstein calves (*Bos taurus*) from The Pirbright Institute (Pirbright) herd were used for these studies. Cannulations were performed essentially as described previously (Hope *et al.*, 2006). Lymph was collected into sterile plastic bottles containing heparin (10 U/ml), penicillin (100 U/ml) and streptomycin (100 μg/ml). The lymph collected was either used fresh or was centrifuged (300 x g, 8 min), resuspended in heat-inactivated foetal calf serum (FCS, Autogen Bioclear) containing 10% DMSO and the cells stored in liquid nitrogen prior to use. Mononuclear cells were isolated from afferent lymph by density gradient centrifugation over Histopaque 1083 (Sigma). *Mycobacterium bovis* Ag85A-specific T cells were obtained from MHC-defined cattle vaccinated subcutaneously with 10^6 CFU of BCG Pasteur. All T cells used were collected 3 weeks post vaccination at the

peak of the response. All animal experiments were approved by the Pirbright's ethics committee and carried out according to the UK Animal (Scientific Procedures) Act 1986.

Cell lines and primary cells.

293 and HeLa cells were obtained and maintained by the Microbiological Services Department (Pirbright) in tissue culture media (TCM) in the absence of antibiotics. CHO cells expressing human recombinant CAR (CHO-CAR) were provided by Dr M. Cottingham, Jenner Institute, University of Oxford, UK. Bovine ALDC (FSC^{high} $MHCII^{+}$ $DEC\text{-}205^{+}$ $CD11c^{+}$ $CD8\alpha^{-}$) were separated from other lymph-migrating cells using a FACSAria II (Becton Dickinson) and purities were confirmed by flow cytometry using FACSDiva v6 (Becton Dickinson). Peripheral blood $CD14^{+}$ monocytes, $CD4^{+}$ and $CD8^{+}$ T cells were magnetically separated using anti-human CD14 (Miltenyi Biotech), CC30 and CC63 mAbs (Guzman *et al.*, 2008) respectively and MACS technology (Miltenyi Biotech, Germany) following the manufacturer's instructions. Typically, the purity of the resulting dendritic and T-cell subsets was over 97% as determined by flow cytometry as described above.

Bovine lung (BL) cells were isolated from Holstein cattle at the time of slaughter and were provided by Pirbright's Microbiological Services Department (Chanter *et al.*, 1986).

Monoclonal antibodies and flow cytometry

Fluorochrome-labelled mouse anti-bovine monoclonal antibodies (mAb) used in this study have been described in detail previously (Brooke *et al.*, 1998; Howard *et al.*, 1991; Howard & Naessens, 1993; Howard *et al.*, 1997; Sallusto *et al.*, 1995). These were CC98-APC (anti-DEC-205), CC14-PE (anti-CD1b), CC149-PerCP/Cy5.5 (anti-SIRPα), IL-A16-AlexaFluor 680/PE (anti-CD11c), IL-A21-PE (anti-MHCII), ILA-88-FITC (anti-MHC I), IL-A156-PE (anti-CD40), N32/52-3 –PE (anti-CD80) IL-A159-PE (anti-CD86), CC30-

APC/Cy5.5 (anti-CD4), CC63-APC/Cy7 (anti-CD8), IL-A111-AlexaFluor 610/PE (anti-CD25), CC302-PE (anti-IFN-γ). Isotype- and concentration-matched anti-turkey rhinotracheitis virus mAbs were used as controls (Hope *et al.*, 2006; Whelan *et al.*, 2003). Dead cells were excluded using the 405 nm excitable dye Live/Dead Aqua or propidium iodide (Invitrogen) following the manufacturer's instructions. The cells were acquired using an LSRFortessa (Becton Dickinson) and staining was analysed using FCS Express v4 (DeNovo Software). Afferent lymph DC were distinguished from other cells on the basis of their high Forward Scatter (FSC), expression of MHC II, CD11c and high intensity expression of DEC-205 and lack of CD8α (Gliddon *et al.*, 2004; Hope *et al.*, 2006). Only live, single events were used for analysis.

Viruses

E1 and E3-deleted recombinant human AdV5 expressing green fluorescent protein (GFP) or mycobacterial antigen 85A (Ag85A) were generated by the Jenner Institute Viral Vector Core Facility, University of Oxford, UK, as described previously (Cubillos-Zapata *et al.*, 2011).

For some assays, aliquots of $1x10^{11}$ vp AdV5 were labelled with NHS-AlexaFluor568, NHS-biotin or NHS-fluorescein (Invitrogen) following the manufacturer's instructions and labelled virus was dialyzed twice against PBS. The virus was then titrated in 293 cells and GFP expression measured by flow cytometry. In some cases the titer was found to be 1 log lower after labelling and the infectious doses were adjusted as required.

Generation of bovine hyperimmune sera to AdV5

Three six month old Holstein-Friesian calves were inoculated intramuscularly with $1x\ 10^{9}$ vp of purified AdV5 three times at six week intervals. The hyperimmune sera used was

447 collected 6 weeks after the last immunization, pooled, and tested in a virus neutralization
448 assay (Sumida *et al.*, 2005).

449 Infection of afferent lymph cells

450 Migrating cells from the afferent lymph were cultured (IMDM containing 10% FCS and 10^{-5}
451 M 2-β-mercaptoethanol (Sigma-Aldrich, Poole, UK) with the recombinant viruses using
452 optimal multiplicities of infection, as described previously (Cubillos-Zapata *et al.*, 2011). In
453 some assays, transferrin-AF568 (Sigma) and dextran-fluorescein (Invitrogen) were used
454 as tracing markers. In neutralization assays, AdV5 was incubated with 1 μg of anti-hexon
455 antibody raised in goats (Millipore) or with bovine pre-immune or hyperimmune sera raised
456 against human AdV5 generated by immunizing calves with $1x10^9$ vp of AdV5 as described
457 above.

458 Detection of known adenovirus receptors and removal from cell surface

459 To analyse the expression of known adenovirus receptors on ALDC and bovine lung cells
460 the following antibodies were used in flow cytometry: N-17 (goat anti-CAR, Santa Cruz
461 Biotechnology), N32/52-3 (anti-CD80), ILA-159 (anti-CD86), IL-A88 (anti-MHC class I), IL-
462 A21 (anti-MHC class II), T320.11 (anti-heparin/heparin sulphate, Merck), 2-2B (anti-sialic
463 acid, Merck), CC30 (anti-CD4), CC63 (anti-CD8), 344519 (anti-CD46, R&D Systems),
464 CCG24 (anti-FcγRII), KD1 (anti-FcγRIII, Abcam), C-20 (anti-DC-SIGN, Santa Cruz
465 Biotechnology), LM609 (anti-$a_v\beta_3$, Chemicon), mAb 2000 (anti-$a_v\beta_1$, Chemicon), 10D5
466 (anti-$a_v\beta_6$, Millipore). All antibodies were obtained from Pirbright except where noted.
467 Antibodies were added to cells (1 μg/10^6 cells) and incubated at 4ºC for 60 min. After 3
468 washes with PBS the cells were stained with AF647-labelled goat, rabbit or mouse-specific
469 secondary antibodies (Serotec) and the cells analysed by flow cytometry as described
470 above.

Digestion of cell surface proteins was achieved using a mixture of proteolytic enzymes (Wald *et al.*, 2001) consisting of 2U of trypsin, 1U of papain, 2U of chymotrypsin (Merck). 10^6 cells were treated with the enzyme mix in a volume of 100 µl for 30 minutes at 37ºC; the cells were then washed twice in cold PBS and resuspended in culture media containing a final concentration of 5 µg/ml of brefeldin A (Sigma).

Virus attachment assay by ELISA

BL cells, ALDC, $CD14^+$ monocytes or 293 cells were cultured on 96-well plates. Antibodies against known AdV5 receptors were added to the cells at 1 µg/10^6 cells; in some cases the following chemical agents known to block AdV5 entry were also added: 10 U of sodium heparin (Sigma), 1 U of trypsin (Sigma), or 10 mM RGD antagonist Cyclo(Ala-Arg-Gly-Asp-3-Aminomethylbenzoyl (Sigma). After 1 hr incubation at 37°C the cells were washed in cold PBS, biotinylated AdV5 (moi=100 vp/cell) was added for 90 minutes on ice or at 37ºC. The cells were then washed three times with ice-cold PBS and fixed with 3% paraformaldehyde (PF). After blocking with 1% bovine serum albumin (BSA) in PBS, streptavidin-HRP (Sigma, 1:500) was added and the plates incubated for 60 min at room temperature. The plates were washed with PBS-Tween and the plates developed with TMB Turbo (Pierce). Reactions were stopped with 1 M H_2SO_4 and optical densities were measured using a FluorostarOptima (BMG Labtech, Germany).

Virus overlay protein binding assay (VOPBA) and Western blot.

VOPBA was carried out essentially as described by (Cao *et al.*, 1998) with a few modifications. Subcellular fractions from 1x10^6 293, BL and ALDC were enriched using the ProteoExtract subcellular fractionation kit (Merk Millipore) following the manufacturer's instructions. Total cell protein and membrane fractions were separated by polyacrylamide gel electrophoresis (PAGE) on 4-10% denaturing and non-denaturing TGX stain-free gels (Bio-Rad) and transferred onto Immun-Blot PVDF membranes (Bio-Rad). The membranes

were blocked with 5% (w/v) dry milk-PBS overnight, rinsed with PBS and probed with AdV5 ($1x10^8$ vp in 10 ml of milk-PBS) for 90 minutes. The membranes were then washed three times with PBS and incubated with 10 μg of biotinylated goat anti-AdV5 (Serotec) in 10 ml of milk-PBS for 60 minutes. The membranes were washed three times and incubated with 10 μg of streptavidin-conjugated horse radish peroxidase (HRP, Dako) in 10 ml of milk-PBS for 60 minutes. After extensive washing, the membranes were developed with Immun-Star WesternC substrate (Bio-Rad) and visualized using a ChemiDocMP digital imager (Bio-Rad). For competition VOPBA and before the addition of AdV5, 10 μg of rabbit anti-CAR pAb (Abcam) was added to the membranes and incubated for 90 min at room temperature. After washing three times with PBS, the membranes were probed with AdV5 and the assay carried out as described above.

For detection of CAR by Western blot, membrane fractions separated by PAGE were transferred onto PVDF membranes, blocked with milk-PBS and probed with 10 μg of rabbit anti-CAR pAb or 1 μg of anti-β actin mouse mAb (Abcam) in 10 ml of milk-PBS. After washing with PBS containing 1% Tween 20 (PBS-T), the membranes were incubated with 1 μg of anti-goat or anti-mouse antibody conjugated to HRP (Dako) in 10 ml of milk-PBS for 60 minutes. After extensive washing with PBS-T, the membranes were developed as described above.

Biochemical inhibitors.

The following inhibitors and final concentrations were used to block endocytosis: cytochalasin D (CCD, 1 μM, actin-dependent (Sakr *et al.*, 2001)); filipin (5 μg/ml caveolae-dependent (Rothberg *et al.*, 1992)); chlorpromazine (CPZ, 10 μg/ml, prevents clathrin-coated pit formation (Wang *et al.*, 1993)); methyl-β-cyclodextrin (mβ-CD, 10 mM, cholesterol-dependent (Vieth *et al.*, 2010)); amiloride (1 mM, Na^+ blocker (West *et al.*,

1989), and therefore blocks macropinocytosis (Sallusto *et al.*, 1995)); ciliobrevin (10 μM, inhibitor of motor cytoplasmatic dynein (Firestone *et al.*, 2012); dynasore (8 mM, inhibitor of dynamin and clathrin-dependent endocytosis (Macia *et al.*, 2006)).

The following lysosomotropic agents were used to block acidification of endosomal compartments: bafilomycin (1 μM, inhibitor of vacuolar-type H^+-ATPase (Yoshimori *et al.*, 1991); NH_4Cl (a weak base (Sonawane *et al.*, 2002) and diluted in PBS); chloroquine (10 μM, inhibits endosomal maturation (Mellman *et al.*, 1986)).

All inhibitors were diluted in dimethyl sulfoxide (DMSO), except where noted. DMSO was used as diluent control and PBS was used as a negative control. All chemicals were obtained from Sigma-Aldrich (Poole, UK). Cells ($1x10^6$ final) were plated in triplicate in culture media in 96 U-bottomed plates, the biochemical inhibitors added to the final concentrations described above in a final volume of 100 µl and mixed thoroughly. After 1hr incubation at 37ºC, virus internalization assays were performed as described below.

Virus internalization assay.

To differentiate between attachment and entry, a fluorometry phagocytosis assay (Wan *et al.*, 1993) based on the capacity of trypan blue to quench extracellular fluorescein was modified. AdV5 was labelled with NHS-fluorescein (Pierce) following the manufacturer's instructions. ALDC or 293 cells were cultured in 96-well plates with the labelled virus (moi=100 vp/cell) for 6 hrs or 60 min respectively at 37ºC or at 4ºC in the presence of the biochemical inhibitors described above. All inhibitors prepared in DMSO were diluted in culture media and 10% DMSO in culture media was used as negative control. After the required incubation period, trypan blue (0.5% final, Sigma) and Live/Dead Aqua (Invitrogen) were added and the cells analysed by flow cytometry; 25,000 live/single events were used to generate statistical analyses.

544 Confocal microscopy

545 FACS purified DC (FSC^{high} $MHCII^+$ $DEC\text{-}205^+$ $CD11c^+$ $CD8\alpha^-$) were cultured on collagen-
546 treated coverslips (Sigma) in the presence (moi = 10) or absence of labelled AdV5. The
547 cells were fixed with 3% paraformaldehyde for 20 minutes, washed twice with PBS and
548 permeabilized with 0.1% Triton X-100 in PBS. Anti-EEA1 polyclonal antibody raised in
549 rabbits (1 μg/ml final concentration, Abcam, UK) was used to visualize early endosomal
550 compartments; the tracer molecules dextran and albumin (both at 0.5 μg/ml final
551 concentration) conjugated to AF488 were used for co-localization assays; rabbit anti-
552 FMDV was used as a negative control (final dilution of 1:750). Goat anti-rabbit-AF488 (1
553 μg/ml, Invitrogen) was used as secondary antibody and all samples were counterstained
554 with DAPI (100 nM, Invitrogen) following the manufacturer's instructions. Where indicated,
555 Phalloidin-AF488 (0.2 U/slide, Invitrogen) was used to identify actin filaments. Cells were
556 mounted onto microscope slides using VectaShield (Vector Laboratories, UK) and
557 observed using a 65x lens mounted on a Leica SP5 confocal microscope. The Leica LAS
558 AF software was used to take sequential, 3D stack images in the Z-plane acquiring stacks
559 of 80 to 120 optical sections from infected cells as optimized by the software. The number
560 of intracellular virions, 3D images and co-localization datasets were analysed using
561 Bitplane Imaris 6.4.2 image analysis software (Bitplane, Switzerland) with surface
562 smoothing of 0.05 nm for nuclei (blue), 0.02 nm for AdV (red) and endosomes (green).

563 pH-dependent fluorometry

564 Dextran-fluorescein (Invitrogen) was used to measure intracellular pH essentially as
565 described previously (Downey *et al.*, 1999). Calibration of the fluorescence ratio versus pH
566 was performed for each experiment by equilibrating the cells in isotonic K^+-rich medium
567 buffered to varying pH values (between 5.0 and 7.5) in the presence of the K^+/H^+
568 ionophore nigericin (5 mM, Sigma). Calibration curves were constructed by plotting the

extracellular pH, which was assumed to be identical to the cytosolic pH under these conditions, against the corresponding fluorescence ratio. AdV5 (moi = 100) or dextran (25 μg/ml) labelled with fluorescein were added to ALDC or 293 cells cultured in triplicate in 96-well plates (Costar). Real time fluorometry was measured every 30 minutes using an Infinite M200 (Tecan) and the results analysed using Magellan for Windows (Tecan).

Generation of oil-in-water emulsions

AdV5 recombinants expressing GFP or Ag85A were mixed with the adjuvant Montanide ISA 206V (SEPPIC, France) to form oil-in-water emulsions following the manufacturer's instructions. Briefly, $1x10^9$ vp in a volume of 250 μl were mixed with an equal volume of adjuvant and vigorously mixed for 2 minutes. Two negative controls were also prepared, one containing AdV5 and adjuvant but without mixing, and the other PBS mixed with ISA 206V and emulsified as described above. The emulsions containing 100 vp/cell were added to 96-well U-bottomed tissue culture plates containing $1x10^5$ ALDC in 100 μl of media and mixed by pipetting until the solution looked homogenous. In the case of the control containing AdV5 and adjuvant without mixing, the solutions were mixed only once and clear hydrophobic/hydrophilic globules observed macroscopically. The infection allowed to continue as described in the text and washed twice with PBS before analysis.

Antigen presentation assays

Ag85A-specific IFN-γ producing lymphocytes were analysed using ELISpot assays as described previously (Guzman *et al.*, 2012; Hope *et al.*, 2012) utilizing purified $CD4^+$ T cells from MHC-matched, BCG-vaccinated animals (Thom *et al.*, 2012).

Statistical analysis

Calculation of descriptive statistics (geometric statistics, standard error of the means and standard deviations), two-way parametric analysis of variants (ANOVA) including multiple

comparisons, Bonferroni multiple comparison tests and graphs were generated using GraphPad Prism for Windows v6.01 (GraphPad, San Diego, CA).

Acknowledgements

We gratefully acknowledge the staff at The Pirbright Institute for care of cattle and the provision of bovine primary cell lines. This work was funded by the Biotechnology and Biological Sciences Research Council BBS/E/I/00001373 and the BBSRC Institute Strategic Programme grant on Livestock Viral Diseases at The Pirbright Institute, United Kingdom. G. Taylor and B. Charleston are Jenner Institute Investigators.

References

Adams, W. C., Bond, E., Havenga, M. J., Holterman, L., Goudsmit, J., Karlsson Hedestam, G. B., Koup, R. A. & Lore, K. (2009). Adenovirus serotype 5 infects human dendritic cells via a coxsackievirus-adenovirus receptor-independent receptor pathway mediated by lactoferrin and DC-SIGN. *J Gen Virol* **90**, 1600-1610.

Ahi, Y. S., Bangari, D. S. & Mittal, S. K. (2011). Adenoviral vector immunity: its implications and circumvention strategies. *Current gene therapy* **11**, 307-320.

Alba, R., Bradshaw, A. C., Parker, A. L., Bhella, D., Waddington, S. N., Nicklin, S. A., van Rooijen, N., Custers, J., Goudsmit, J., Barouch, D. H., McVey, J. H. & Baker, A. H. (2009). Identification of coagulation factor (F)X binding sites on the adenovirus serotype 5 hexon: effect of mutagenesis on FX interactions and gene transfer. *Blood* **114**, 965-971.

Ashbourne Excoffon, K. J., Moninger, T. & Zabner, J. (2003). The coxsackie B virus and adenovirus receptor resides in a distinct membrane microdomain. *J Virol* **77**, 2559-2567.

Bergelson, J. M., Cunningham, J. A., Droguett, G., Kurt-Jones, E. A., Krithivas, A., Hong, J. S., Horwitz, M. S., Crowell, R. L. & Finberg, R. W. (1997). Isolation of a common receptor for Coxsackie B viruses and adenoviruses 2 and 5. *Science* **275**, 1320-1323.

Bremner, K. H., Scherer, J., Yi, J., Vershinin, M., Gross, S. P. & Vallee, R. B. (2009). Adenovirus transport via direct interaction of cytoplasmic dynein with the viral capsid hexon subunit. *Cell host & microbe* **6**, 523-535.

Brooke, G. P., Parsons, K. R. & Howard, C. J. (1998). Cloning of two members of the SIRP alpha family of protein tyrosine phosphatase binding proteins in cattle that are expressed on monocytes and a subpopulation of dendritic cells and which mediate binding to CD4 T cells. *Eur J Immunol* **28**, 1-11.

Burckhardt, C. J., Suomalainen, M., Schoenenberger, P., Boucke, K., Hemmi, S. & Greber, U. F. (2011). Drifting motions of the adenovirus receptor CAR and immobile integrins initiate virus uncoating and membrane lytic protein exposure. *Cell host & microbe* **10**, 105-117.

Cao, W., Henry, M. D., Borrow, P., Yamada, H., Elder, J. H., Ravkov, E. V., Nichol, S. T., Compans, R. W., Campbell, K. P. & Oldstone, M. B. (1998). Identification of alpha-dystroglycan as a receptor for lymphocytic choriomeningitis virus and Lassa fever virus. *Science* **282**, 2079-2081.

Chanter, N., Rutter, J. M. & Luther, P. D. (1986). Rapid detection of toxigenic Pasteurella multocida by an agar overlay method. *Vet Rec* **119**, 629-630.

Chen, C. L., Hou, W. H., Liu, I. H., Hsiao, G., Huang, S. S. & Huang, J. S. (2009). Inhibitors of clathrin-dependent endocytosis enhance TGFbeta signaling and responses. *Journal of cell science* **122**, 1863-1871.

Chen, R. F. & Lee, C. Y. (2014). Adenoviruses types, cell receptors and local innate cytokines in adenovirus infection. *International reviews of immunology* **33**, 45-53.

Christoforidis, S., McBride, H. M., Burgoyne, R. D. & Zerial, M. (1999). The Rab5 effector EEA1 is a core component of endosome docking. *Nature* **397**, 621-625.

Cooper, J. A. (1987). Effects of cytochalasin and phalloidin on actin. *J Cell Biol* **105**, 1473-1478.

Cubillos-Zapata, C., Guzman, E., Turner, A., Gilbert, S. C., Prentice, H., Hope, J. C. & Charleston, B. (2011). Differential effects of viral vectors on migratory afferent lymph dendritic cells in vitro predict enhanced immunogenicity in vivo. *J Virol* **85**, 9385-9394.

de Vries, E., Tscherne, D. M., Wienholts, M. J., Cobos-Jimenez, V., Scholte, F., Garcia-Sastre, A., Rottier, P. J. & de Haan, C. A. (2011). Dissection of the influenza A virus endocytic routes reveals macropinocytosis as an alternative entry pathway. *PLoS Pathog* **7**, e1001329.

Dicks, M. D., Guzman, E., Spencer, A. J., Gilbert, S. C., Charleston, B., Hill, A. V. & Cottingham, M. G. (2015). The relative magnitude of transgene-specific adaptive immune responses induced by human and chimpanzee adenovirus vectors differs between laboratory animals and a target species. *Vaccine* **33**, 1121-1128.

Downey, G. P., Botelho, R. J., Butler, J. R., Moltyaner, Y., Chien, P., Schreiber, A. D. & Grinstein, S. (1999). Phagosomal maturation, acidification, and inhibition of bacterial growth in nonphagocytic cells transfected with FcgammaRIIA receptors. *J Biol Chem* **274**, 28436-28444.

Ellis, S. A., Staines, K. A. & Morrison, W. I. (1996). cDNA sequence of cattle MHC class I genes transcribed in serologically defined haplotypes A18 and A31. *Immunogenetics* **43**, 156-159.

Ellis, S. A., Staines, K. A., Stear, M. J., Hensen, E. J. & Morrison, W. I. (1998). DNA typing for BoLA class I using sequence-specific primers (PCR-SSP). *Eur J Immunogenet* **25**, 365-370.

Firestone, A. J., Weinger, J. S., Maldonado, M., Barlan, K., Langston, L. D., O'Donnell, M., Gelfand, V. I., Kapoor, T. M. & Chen, J. K. (2012). Small-molecule inhibitors of the AAA+ ATPase motor cytoplasmic dynein. *Nature* **484**, 125-129.

Ganne, V., Eloit, M., Laval, A., Adam, M. & Trouve, G. (1994). Enhancement of the efficacy of a replication-defective adenovirus-vectored vaccine by the addition of oil adjuvants. *Vaccine* **12**, 1190-1196.

Gliddon, D. R., Hope, J. C., Brooke, G. P. & Howard, C. J. (2004). DEC-205 expression on migrating dendritic cells in afferent lymph. *Immunology* **111**, 262-272.

Gliddon, D. R. & Howard, C. J. (2002). CD26 is expressed on a restricted subpopulation of dendritic cells in vivo. *Eur J Immunol* **32**, 1472-1481.

Greber, U. F., Willetts, M., Webster, P. & Helenius, A. (1993). Stepwise dismantling of adenovirus 2 during entry into cells. *Cell* **75**, 477-486.

Green, C. A., Scarselli, E., Sande, C. J., Thompson, A. J., de Lara, C. M., Taylor, K. S., Haworth, K., Del Sorbo, M., Angus, B., Siani, L., Di Marco, S., Traboni, C., Folgori, A., Colloca, S., Capone, S., Vitelli, A., Cortese, R., Klenerman, P., Nicosia, A. & Pollard, A. J. (2015). Chimpanzee adenovirus- and MVA-vectored respiratory syncytial virus vaccine is safe and immunogenic in adults. *Science translational medicine* **7**, 300ra126.

Guzman, E., Cubillos-Zapata, C., Cottingham, M. G., Gilbert, S. C., Prentice, H., Charleston, B. & Hope, J. C. (2012). Modified vaccinia virus Ankara-based vaccine vectors induce apoptosis in dendritic cells draining from the skin via both the extrinsic and intrinsic caspase pathways, preventing efficient antigen presentation. *J Virol* **86**, 5452-5466.

Guzman, E., Taylor, G., Charleston, B., Skinner, M. A. & Ellis, S. A. (2008). An MHC-restricted CD8+ T-cell response is induced in cattle by foot-and-mouth disease virus (FMDV) infection and also following vaccination with inactivated FMDV. *J Gen Virol* **89**, 667-675.

Hemati, B., Contreras, V., Urien, C., Bonneau, M., Takamatsu, H. H., Mertens, P. P., Breard, E., Sailleau, C., Zientara, S. & Schwartz-Cornil, I. (2009). Bluetongue virus targets conventional dendritic cells in skin lymph. *J Virol* **83**, 8789-8799.

Hope, J. C., Guzman, E., Cubillos-Zapata, C., Stephens, S. A., Gilbert, S. C., Prentice, H., Sopp, P., Howard, C. J. & Charleston, B. (2012). Migratory sub-populations of afferent lymphatic dendritic cells differ in their interactions with Mycobacterium bovis Bacille Calmette Guerin. *Vaccine* **30**, 2357-2367.

Hope, J. C., Howard, C. J., Prentice, H. & Charleston, B. (2006). Isolation and purification of afferent lymph dendritic cells that drain the skin of cattle. *Nat Protoc* **1**, 982-987.

Howard, C. J., Morrison, W. I., Bensaid, A., Davis, W., Eskra, L., Gerdes, J., Hadam, M., Hurley, D., Leibold, W., Letesson, J. J. & et al. (1991). Summary of workshop findings for leukocyte antigens of cattle. *Vet Immunol Immunopathol* **27**, 21-27.

Howard, C. J. & Naessens, J. (1993). Summary of workshop findings for cattle (tables 1 and 2). *Vet Immunol Immunopathol* **39**, 25-47.

Howard, C. J., Sopp, P., Brownlie, J., Kwong, L. S., Parsons, K. R. & Taylor, G. (1997). Identification of two distinct populations of dendritic cells in afferent lymph that vary in their ability to stimulate T cells. *J Immunol* **159**, 5372-5382.

Huang, S., Kamata, T., Takada, Y., Ruggeri, Z. M. & Nemerow, G. R. (1996). Adenovirus interaction with distinct integrins mediates separate events in cell entry and gene delivery to hematopoietic cells. *J Virol* **70**, 4502-4508.

Jindadamrongwech, S. & Smith, D. R. (2004). Virus Overlay Protein Binding Assay (VOPBA) reveals serotype specific heterogeneity of dengue virus binding proteins on HepG2 human liver cells. *Intervirology* **47**, 370-373.

Kalyuzhniy, O., Di Paolo, N. C., Silvestry, M., Hofherr, S. E., Barry, M. A., Stewart, P. L. & Shayakhmetov, D. M. (2008). Adenovirus serotype 5 hexon is critical for virus infection of hepatocytes in vivo. *Proc Natl Acad Sci U S A* **105**, 5483-5488.

Karger, A. & Mettenleiter, T. C. (1996). Identification of cell surface molecules that interact with pseudorabies virus. *J Virol* **70**, 2138-2145.

Macia, E., Ehrlich, M., Massol, R., Boucrot, E., Brunner, C. & Kirchhausen, T. (2006). Dynasore, a cell-permeable inhibitor of dynamin. *Developmental cell* **10**, 839-850.

Mallery, D. L., McEwan, W. A., Bidgood, S. R., Towers, G. J., Johnson, C. M. & James, L. C. (2010). Antibodies mediate intracellular immunity through tripartite motif-containing 21 (TRIM21). *Proc Natl Acad Sci U S A* **107**, 19985-19990.

Meier, O., Gastaldelli, M., Boucke, K., Hemmi, S. & Greber, U. F. (2005). Early steps of clathrin-mediated endocytosis involved in phagosomal escape of Fcgamma receptor-targeted adenovirus. *J Virol* **79**, 2604-2613.

Mellman, I., Fuchs, R. & Helenius, A. (1986). Acidification of the endocytic and exocytic pathways. *Annual review of biochemistry* **55**, 663-700.

Otero, M. J. & Carrasco, L. (1987). Proteins are cointernalized with virion particles during early infection. *Virology* **160**, 75-80.

Platt, C. D., Ma, J. K., Chalouni, C., Ebersold, M., Bou-Reslan, H., Carano, R. A., Mellman, I. & Delamarre, L. (2010). Mature dendritic cells use endocytic receptors to capture and present antigens. *Proc Natl Acad Sci U S A* **107**, 4287-4292.

Puntener, D., Engelke, M. F., Ruzsics, Z., Strunze, S., Wilhelm, C. & Greber, U. F. (2011). Stepwise loss of fluorescent core protein V from human adenovirus during entry into cells. *J Virol* **85**, 481-496.

Rodriguez, E. & Everitt, E. (1996). Adenovirus uncoating and nuclear establishment are not affected by weak base amines. *J Virol* **70**, 3470-3477.

Rossi, M. & Young, J. W. (2005). Human dendritic cells: potent antigen-presenting cells at the crossroads of innate and adaptive immunity. *J Immunol* **175**, 1373-1381.

Rothberg, K. G., Heuser, J. E., Donzell, W. C., Ying, Y. S., Glenney, J. R. & Anderson, R. G. (1992). Caveolin, a protein component of caveolae membrane coats. *Cell* **68**, 673-682.

Roy, S., Clawson, D. S., Calcedo, R., Lebherz, C., Sanmiguel, J., Wu, D. & Wilson, J. M. (2005). Use of chimeric adenoviral vectors to assess capsid neutralization determinants. *Virology* **333**, 207-214.

Sakr, S. W., Eddy, R. J., Barth, H., Wang, F., Greenberg, S., Maxfield, F. R. & Tabas, I. (2001). The uptake and degradation of matrix-bound lipoproteins by macrophages

require an intact actin Cytoskeleton, Rho family GTPases, and myosin ATPase activity. *J Biol Chem* **276**, 37649-37658.

Sallusto, F., Cella, M., Danieli, C. & Lanzavecchia, A. (1995). Dendritic cells use macropinocytosis and the mannose receptor to concentrate macromolecules in the major histocompatibility complex class II compartment: downregulation by cytokines and bacterial products. *J Exp Med* **182**, 389-400.

Sandgren, K. J., Wilkinson, J., Miranda-Saksena, M., McInerney, G. M., Byth-Wilson, K., Robinson, P. J. & Cunningham, A. L. (2010). A differential role for macropinocytosis in mediating entry of the two forms of vaccinia virus into dendritic cells. *PLoS Pathog* **6**, e1000866.

Savina, A. & Amigorena, S. (2007). Phagocytosis and antigen presentation in dendritic cells. *Immunol Rev* **219**, 143-156.

Schwartz-Cornil, I., Epardaud, M. & Bonneau, M. (2006). Cervical duct cannulation in sheep for collection of afferent lymph dendritic cells from head tissues. *Nat Protoc* **1**, 874-879.

Sirena, D., Lilienfeld, B., Eisenhut, M., Kalin, S., Boucke, K., Beerli, R. R., Vogt, L., Ruedl, C., Bachmann, M. F., Greber, U. F. & Hemmi, S. (2004). The human membrane cofactor CD46 is a receptor for species B adenovirus serotype 3. *J Virol* **78**, 4454-4462.

Smith, J. G., Cassany, A., Gerace, L., Ralston, R. & Nemerow, G. R. (2008). Neutralizing antibody blocks adenovirus infection by arresting microtubule-dependent cytoplasmic transport. *J Virol* **82**, 6492-6500.

Smith, J. G., Wiethoff, C. M., Stewart, P. L. & Nemerow, G. R. (2010). Adenovirus. *Curr Top Microbiol Immunol* **343**, 195-224.

Sonawane, N. D., Thiagarajah, J. R. & Verkman, A. S. (2002). Chloride concentration in endosomes measured using a ratioable fluorescent Cl- indicator: evidence for chloride accumulation during acidification. *J Biol Chem* **277**, 5506-5513.

Steinman, R. M. (1991). The dendritic cell system and its role in immunogenicity. *Annu Rev Immunol* **9**, 271-296.

Steinman, R. M. & Cohn, Z. A. (1973). Identification of a novel cell type in peripheral lymphoid organs of mice. I. Morphology, quantitation, tissue distribution. *J Exp Med* **137**, 1142-1162.

Sumida, S. M., Truitt, D. M., Lemckert, A. A., Vogels, R., Custers, J. H., Addo, M. M., Lockman, S., Peter, T., Peyerl, F. W., Kishko, M. G., Jackson, S. S., Gorgone, D. A., Lifton, M. A., Essex, M., Walker, B. D., Goudsmit, J., Havenga, M. J. & Barouch, D. H. (2005). Neutralizing antibodies to adenovirus serotype 5 vaccine vectors are directed primarily against the adenovirus hexon protein. *J Immunol* **174**, 7179-7185.

Suomalainen, M., Luisoni, S., Boucke, K., Bianchi, S., Engel, D. A. & Greber, U. F. (2013). A direct and versatile assay measuring membrane penetration of adenovirus in single cells. *J Virol* **87**, 12367-12379.

Svensson, U. & Persson, R. (1984). Entry of adenovirus 2 into HeLa cells. *J Virol* **51**, 687-694.

Taylor, G., Thom, M., Capone, S., Pierantoni, A., Guzman, E., Herbert, R., Scarselli, E., Napolitano, F., Giuliani, A., Folgori, A., Colloca, S., Cortese, R., Nicosia, A. & Vitelli, A. (2015). Efficacy of a virus-vectored vaccine against human and bovine respiratory syncytial virus infections. *Science translational medicine* **7**, 300ra127.

Tayyari, F., Marchant, D., Moraes, T. J., Duan, W., Mastrangelo, P. & Hegele, R. G. (2011). Identification of nucleolin as a cellular receptor for human respiratory syncytial virus. *Nat Med* **17**, 1132-1135.

Thom, M. L., McAulay, M., Vordermeier, H. M., Clifford, D., Hewinson, R. G., Villarreal-Ramos, B. & Hope, J. C. (2012). Duration of immunity against

Mycobacterium bovis following neonatal vaccination with bacillus Calmette-Guerin Danish: significant protection against infection at 12, but not 24, months. *Clin Vaccine Immunol* **19**, 1254-1260.

Vieth, J. A., Kim, M. K., Pan, X. Q., Schreiber, A. D. & Worth, R. G. (2010). Differential requirement of lipid rafts for FcgammaRIIA mediated effector activities. *Cell Immunol* **265**, 111-119.

Waddington, S. N., McVey, J. H., Bhella, D., Parker, A. L., Barker, K., Atoda, H., Pink, R., Buckley, S. M., Greig, J. A., Denby, L., Custers, J., Morita, T., Francischetti, I. M., Monteiro, R. Q., Barouch, D. H., van Rooijen, N., Napoli, C., Havenga, M. J., Nicklin, S. A. & Baker, A. H. (2008). Adenovirus serotype 5 hexon mediates liver gene transfer. *Cell* **132**, 397-409.

Wald, M., Olejar, T., Sebkova, V., Zadinova, M., Boubelik, M. & Pouckova, P. (2001). Mixture of trypsin, chymotrypsin and papain reduces formation of metastases and extends survival time of C57Bl6 mice with syngeneic melanoma B16. *Cancer chemotherapy and pharmacology* **47 Suppl**, S16-22.

Wan, C. P., Park, C. S. & Lau, B. H. (1993). A rapid and simple microfluorometric phagocytosis assay. *J Immunol Methods* **162**, 1-7.

Wang, L. H., Rothberg, K. G. & Anderson, R. G. (1993). Mis-assembly of clathrin lattices on endosomes reveals a regulatory switch for coated pit formation. *J Cell Biol* **123**, 1107-1117.

West, M. A., Bretscher, M. S. & Watts, C. (1989). Distinct endocytotic pathways in epidermal growth factor-stimulated human carcinoma A431 cells. *J Cell Biol* **109**, 2731-2739.

Whelan, A. O., Hope, J. C., Howard, C. J., Clifford, D., Hewinson, R. G. & Vordermeier, H. M. (2003). Modulation of the bovine delayed-type hypersensitivity responses to defined mycobacterial antigens by a synthetic bacterial lipopeptide. *Infect Immun* **71**, 6420-6425.

Wiethoff, C. M., Wodrich, H., Gerace, L. & Nemerow, G. R. (2005). Adenovirus protein VI mediates membrane disruption following capsid disassembly. *J Virol* **79**, 1992-2000.

Wolfrum, N. & Greber, U. F. (2013). Adenovirus signalling in entry. *Cellular microbiology* **15**, 53-62.

Yoshimori, T., Yamamoto, A., Moriyama, Y., Futai, M. & Tashiro, Y. (1991). Bafilomycin A1, a specific inhibitor of vacuolar-type H(+)-ATPase, inhibits acidification and protein degradation in lysosomes of cultured cells. *J Biol Chem* **266**, 17707-17712.

Zhang, Y. & Bergelson, J. M. (2005). Adenovirus receptors. *J Virol* **79**, 12125-12131.

FIGURE LEGENDS

Figure 1. Phenotype of ALDC and expression of CAR in bovine cells. a) The phenotype of ALDC was characterized as FSC^{high} MHC class II^+ $DEC205^+$ $CD11c^+$ $CD8\alpha^-$ and 91% of these cells were $CD172a^+$. The plot is representative of all samples analysed (n = 8 animals). b) Expression of CAR and β-actin was assessed by Western blot on enriched membrane fractions from 293, bovine lung (BL) or ALDC. Blot representative of 3 different experiments. c and d) Virus overlay protein binding assay (VOPBA) was used to confirm binding of AdV5 to enriched membrane fractions from 293 and BL but not from ALDC under denaturing and non-denaturing conditions. e) Competition VOPBA using anti-CAR antibodies to block binding of AdV5 to enriched membrane fractions from 293 and BL cells. Blots representative of 5 different experiments.

Figure 2. Transduction of ALDC by AdV5-GFP following removal of putative receptors from the cells' surface. a-f) Expression of putative AdV5 receptors on ALDC 24 hrs after treatment (doted histograms) or mock treatment (solid histograms); grey-filled histograms: isotype controls. g-l) Expression of GFP in AdV5-GFP transduced untreated (solid histograms), treated (doted histograms) or mock transduced ALDC (grey-filled histograms). m and n) Expression of GFP in AdV5-GFP-transduced ALDC and 293 cells in the presence of the RGD antagonist Cyclo(Ala-Arg-Gly-Asp-3-Aminomethylbenzoyl (doted histogram) or control peptide (solid histogram); grey-filled histogram: mock transduced cells. o and p) Expression of GFP in AdV5-GFP-transduced ALDC and 293 in the presence of AdV5-hyperimmune bovine sera (doted histograms), normal bovine serum (solid histograms) or mock transduced (grey-filled histograms). Plots are representative of cells from 6 different animals analysed in duplicate.

Figure 3. AdV5 entry and trans-gene expression in ALDC is significantly different from that in CAR-expressing 293 cells. ALDC (white circles) and 293 cells (black squares) were cultured on ice (4^{o}C) or at 37ºC with biotinylated AdV5-GFP for 90 minutes followed by washing off the inoculum. a) Biotinylated membrane-bound virus was detected by ELISA using streptavidin-HRP. b) Cells were transduced as before and cultured for 24 hrs at 37ºC; expression of the trans-gene (GFP) was detected by flow cytometry. c) ALDC and 293 cells were cultured at 37ºC in the presence of AdV5-GFP. At 1 hr intervals, aliquots were washed with PBS and the cells allowed to recover overnight after which GFP expression was measured by flow cytometry. d) ALDC and 293 cells were cultured at 37ºC in the presence of AdV5-GFP and without washing; GFP expression was measured by flow cytometry at 1 hr intervals. Each point represents the mean of cells from 6 different animals tested in duplicate and error bars indicate standard error of the mean.

Figure 4. Uptake of AdV in DC is blocked by inhibitors of actin-dependent endocytosis. ALDC and 293 cells were cultured with AdV5-Fluo for 1 hr at 37ºC in the presence of various endocytosis inhibitors as described in materials and methods. Extracellular fluorescein was then quenched with trypan blue and fluorescence was measured by flow cytometry. A) Representative histograms showing fluorescence after various treatments. The markers indicate percentage of fluorescein-positive cells above background. b) Bar graphs showing means and standard deviations of the percentage of fluorescein^{+} ALDC obtained from 6 different animals and tested in duplicate or 293 cells tested in triplicate. Asterisks indicate *=$p<0.05$ and **=$p<0.005$ compared to treatment with DMSO.

Figure 5. Entry of AdV5 into ALDC. ALDC were cultured at 37ºC in the presence of AF568-labelled AdV5 (moi = 100). Cells were fixed and analysed by confocal microscopy at 3 hrs (a) 4hr (b) or 5 hrs (d) post infection. Blue: DAPI; Green: Phalloidin-AF488 (for F-

actin); Red: AdV5-AF568. Representative samples of cells from 5 different animals. The scale bar represents 20 μm.

Figure 6. The majority of AdV are not associated with early endosomes. ALDC were cultured with AdV5-AF568 (red) and Dextran-AF488 (green) or albumin-AF488 (green) for 4 hrs and fixed. The early endosome marker (EEA1) was detected using monospecific antibodies and AF488 secondary antibodies (green) as described in Materials and Methods and the samples analysed by confocal microscopy. a) Colocalization of AdV5 and EEA1; b) AdV5 and dextran; d) AdV5 and albumin. Blue: DAPI; Yellow: co-localization. Inserts show a higher magnification of the region of interest. Arrows indicate colocalization events. Representative samples cells from 4 different animals. d) Bar graph showing mean percentage of co-localization voxels from single-slice histograms across the Z-plane from at least 10 confocal images processed from cells from 4 different animals. Error bars indicate standard error of the mean.

Figure 7. Acidification of endosomes is not required for transduction of ALDC by AdV5. a) ALDC or 293 cells were incubated with AdV5-GFP for 24 hrs in the presence of various inhibitors of intracellular acidic microenvironment or with the diluents DMSO or PBS. Trans-gene expression (GFP) was measured by flow cytometry. b) ALDC were cultured at 37ºC with fluorescein-labelled AdV5 or dextran for 4 hrs in the presence of normal tissue culture media or media containing 10 mM NH_4Cl pH 7.5. After washing fluorescein mean fluorescence intensity (MFI) was measured by flow cytometry. c) Relative fluorescence standard curve of fluorescein-dextran at various pH. D) ALDC were cultured in the presence of fluorescein-labelled AdV5 or dextran. Relative fluorescence (RFU) was measured by real time fluorometry. Each point represents the mean of cells from 4 different animals tested in duplicate and error bars indicate standard error of the mean.

Figure 8. Oil-in-water adjuvants improve AdV5 uptake by ALDC, increase and prolong recombinant antigen expression and enhance antigen presentation. AF568-labelled AdV5 was mixed with PBS or an oil-in-water adjuvant, added to ALDC, cultured overnight and washed twice prior to analysis. a) Confocal microscopy was used to count the number of intracellular virions/cell 4 hrs post infection. b and c) 3D reconstructions of representative samples of ALDC infected with AdV5-568 in PBS or adjuvant respectively 4 hrs post infection. d) GFP mean fluorescence intensity (MFI) of ALDC infected with AdV5-GFP in PBS or adjuvant 24 hrs post infection. e) Frequency of GFP-expressing ALDC over time following infection with AdV5-GFP in PBS or adjuvant. f) Ag85A-specific IFN-γ ELISpot using AdV5-Ag85A or AdV5-GFP in PBS or adjuvant. ALDC were infected with AdV5 recombinants as described in Materials and Methods and cultured with MHC-matched $CD4^+$ T cells from BCG-vaccinated animals. In all cases the bars indicate means of 20 imaged cells from 3 different animals analysed in duplicate and error bars indicate standard error of the means.

Figure 1

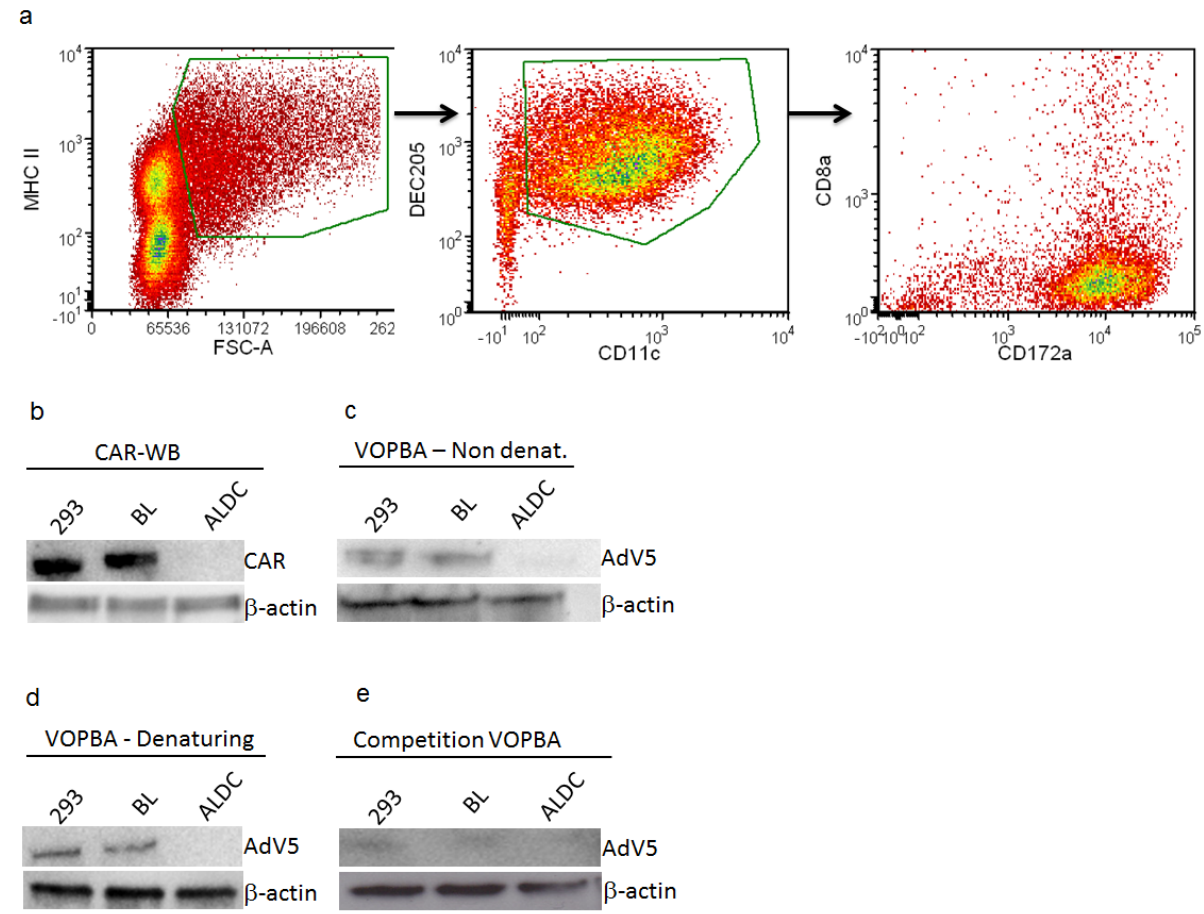
a
MHC II
FSC-A
DEC205
CD11c
CD8a
CD172a
b
CAR-WB
293
BL
ALDC
CAR
β-actin
c
VOPBA – Non denat.
AdV5
d
VOPBA - Denaturing
e
Competition VOPBA

Figure 2

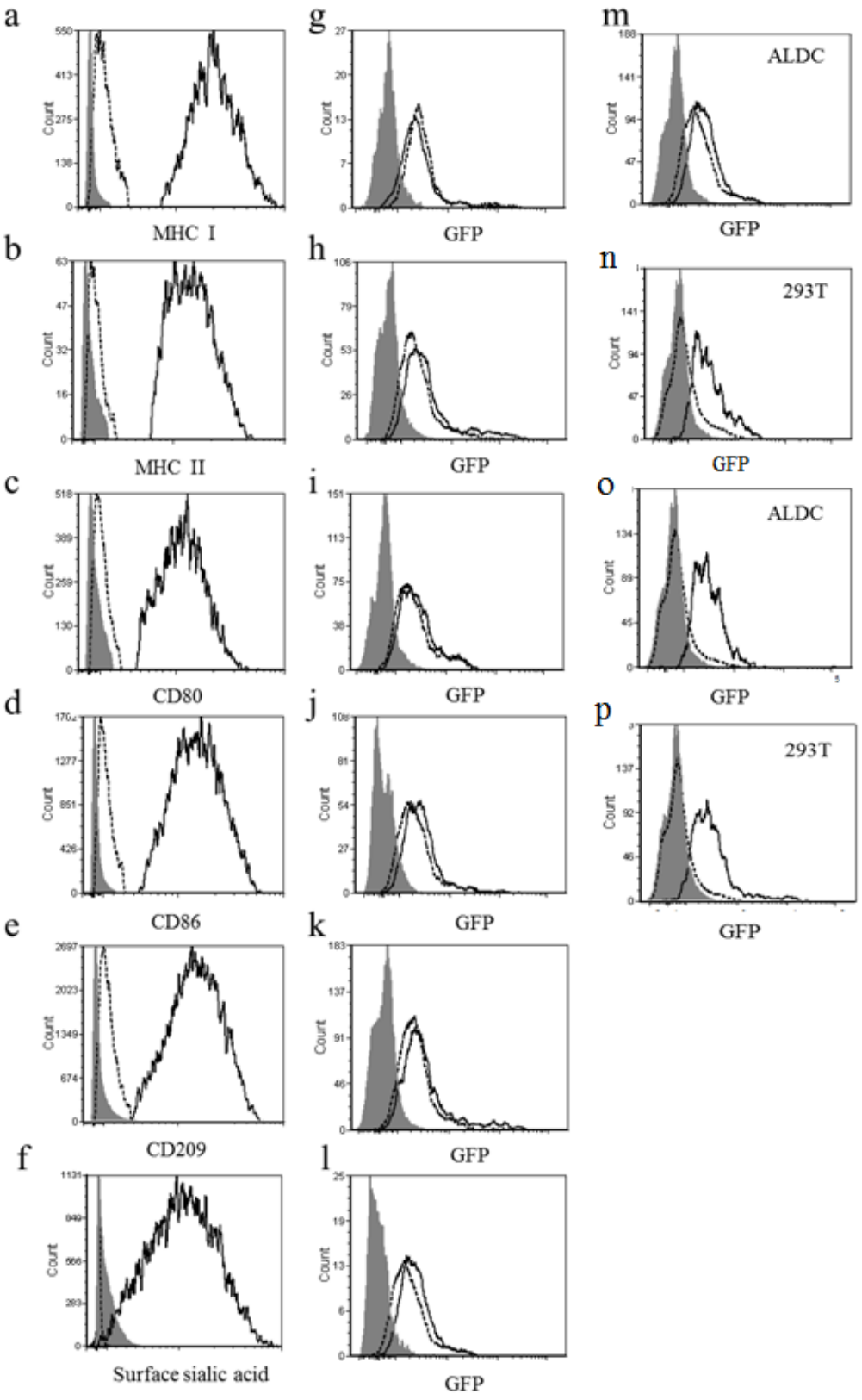
a
MHC I
b
MHC II
c
CD80
d
CD86
e
CD209
f
Surface sialic acid
g
GFP
h
GFP
i
GFP
j
GFP
k
GFP
l
GFP
m
ALDC
GFP
n
293T
GFP
o
ALDC
GFP
p
293T
GFP
Count

Figure 3

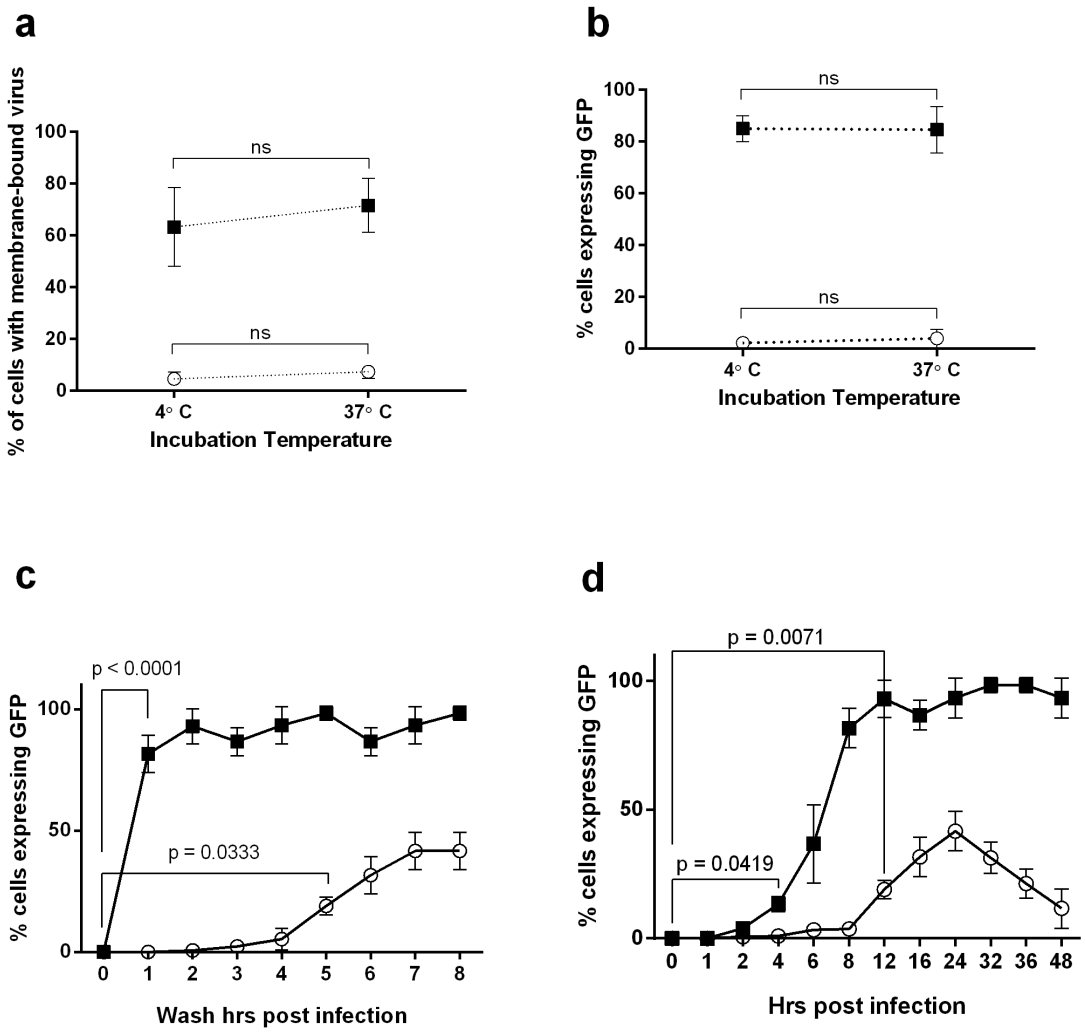
a
% of cells with membrane-bound virus
100
80
60
40
20
0
ns
ns
4° C
37° C
Incubation Temperature
b
% cells expressing GFP
100
80
60
40
20
0
ns
ns
4° C
37° C
Incubation Temperature
c
% cells expressing GFP
p < 0.0001
p = 0.0333
100
50
0
0 1 2 3 4 5 6 7 8
Wash hrs post infection
d
% cells expressing GFP
p = 0.0071
p = 0.0419
100
50
0
0 1 2 4 6 8 12 16 24 32 36 48
Hrs post infection

Figure 4

a

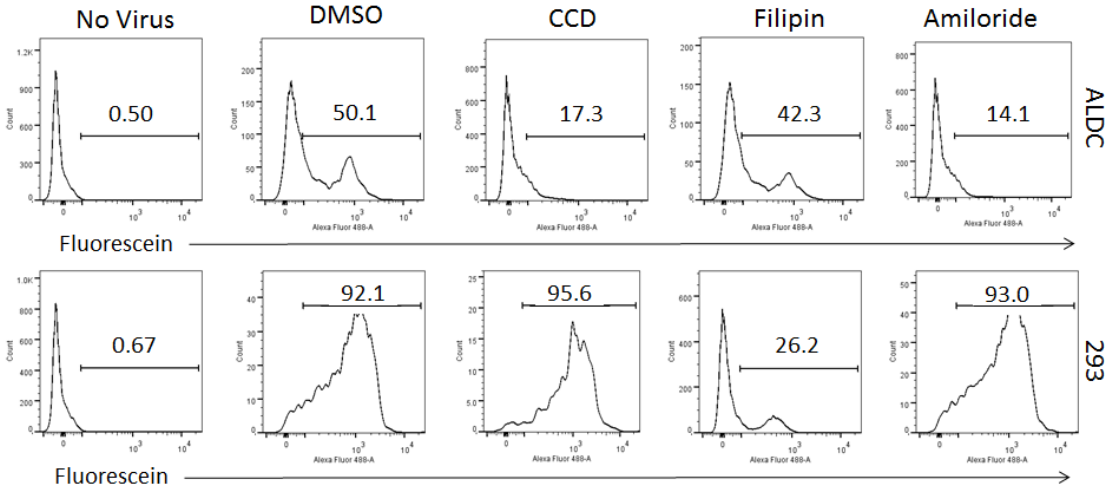
No Virus
DMSO
CCD
Filipin
Amiloride
0.50
50.1
17.3
42.3
14.1
ALDC
Fluorescein
0.67
92.1
95.6
26.2
93.0
293
Fluorescein

b

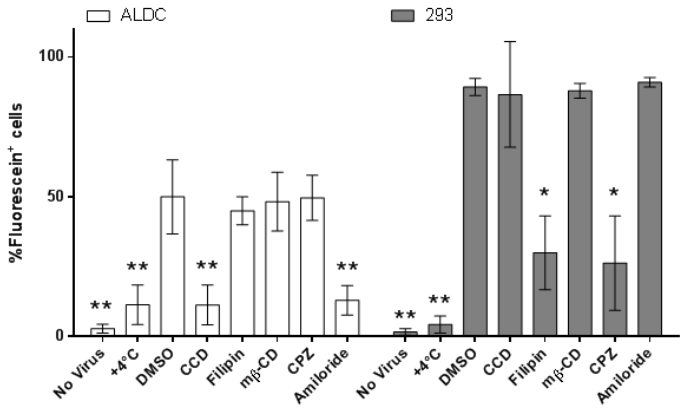
ALDC
293
%Fluorescein+ cells
100
50
0
No Virus
+4°C
DMSO
CCD
Filipin
mβ-CD
CPZ
Amiloride

Figure 5

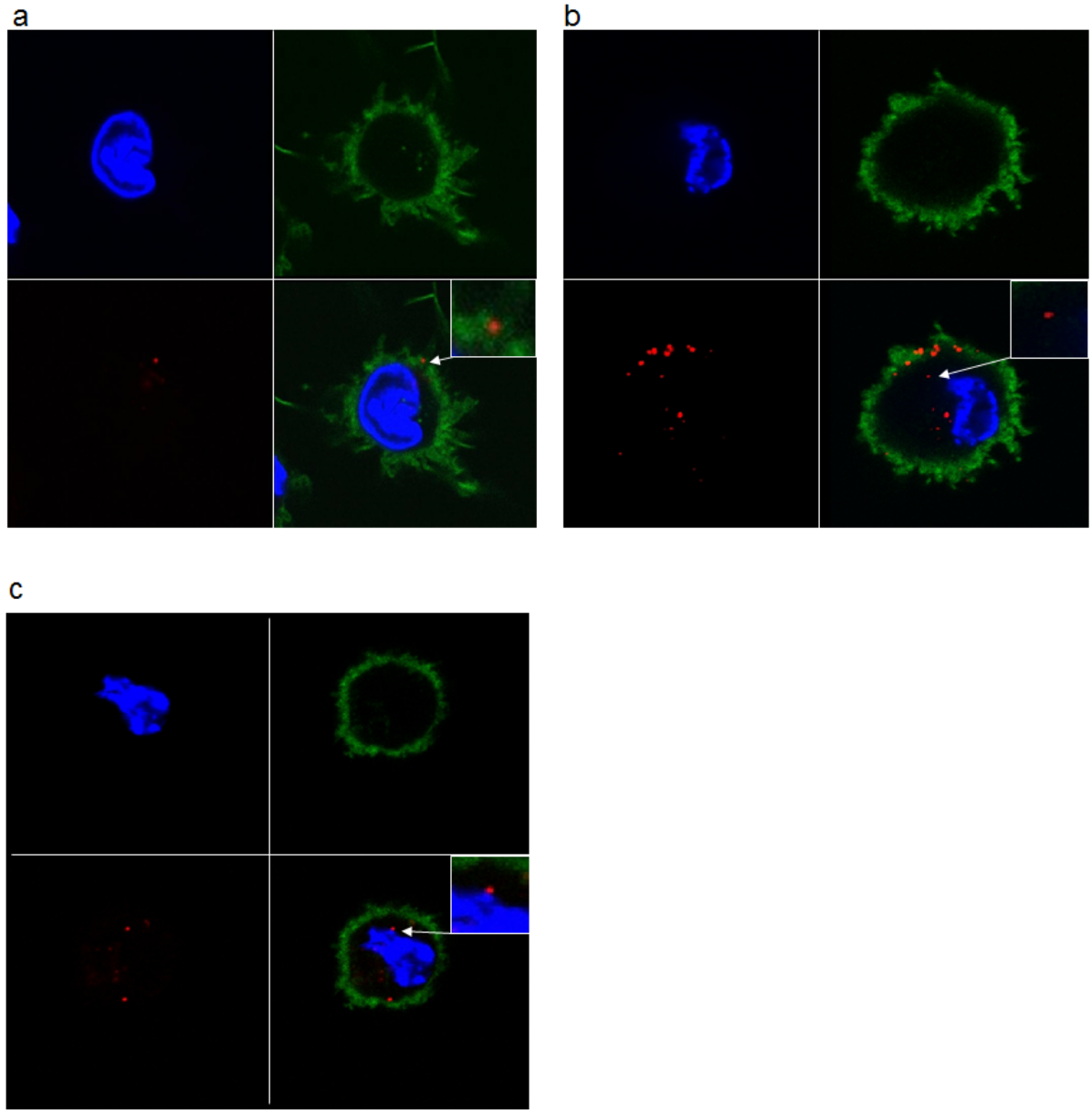

Figure 6

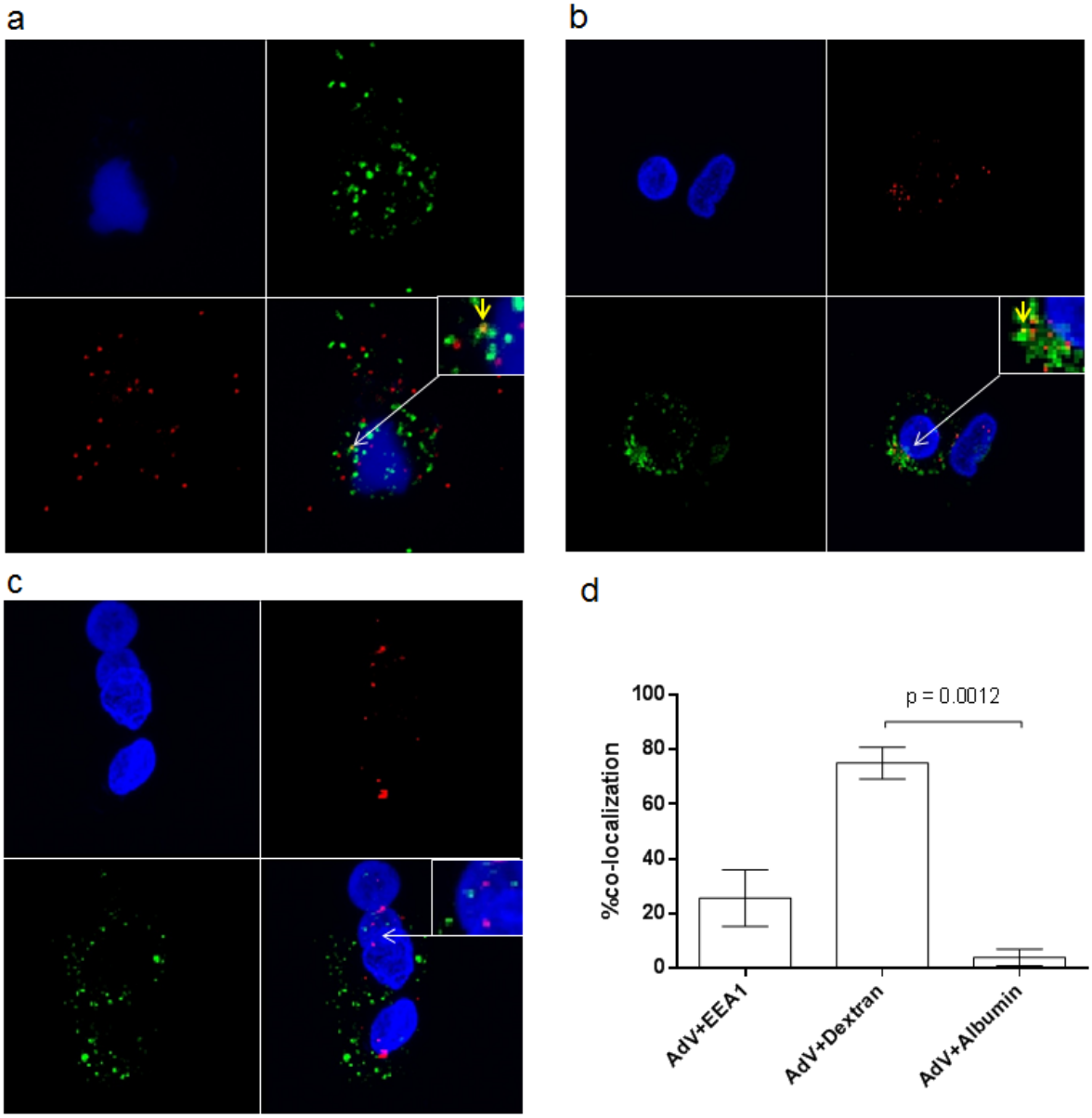
a
b
c
d
p = 0.0012
%co-localization
100
80
60
40
20
0
AdV+EEA1
AdV+Dextran
AdV+Albumin

Figure 7

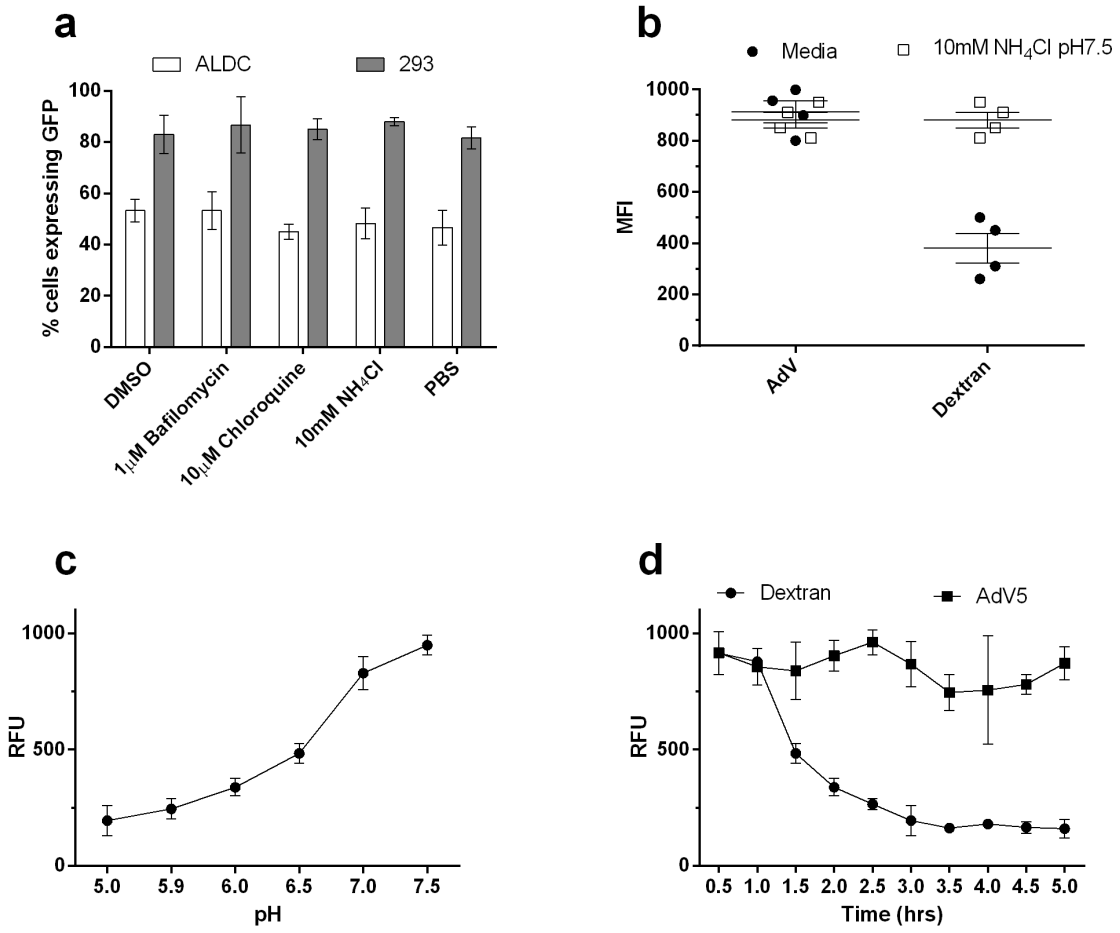
a
ALDC
293
% cells expressing GFP
100
80
60
40
20
0
DMSO
1μM Bafilomycin
10μM Chloroquine
10mM NH4Cl
PBS
b
Media
10mM NH4Cl pH7.5
MFI
1000
800
600
400
200
0
AdV
Dextran
c
RFU
1000
500
0
5.0
5.9
6.0
6.5
7.0
7.5
pH
d
Dextran
AdV5
RFU
1000
500
0
0.5
1.0
1.5
2.0
2.5
3.0
3.5
4.0
4.5
5.0
Time (hrs)

Figure 8

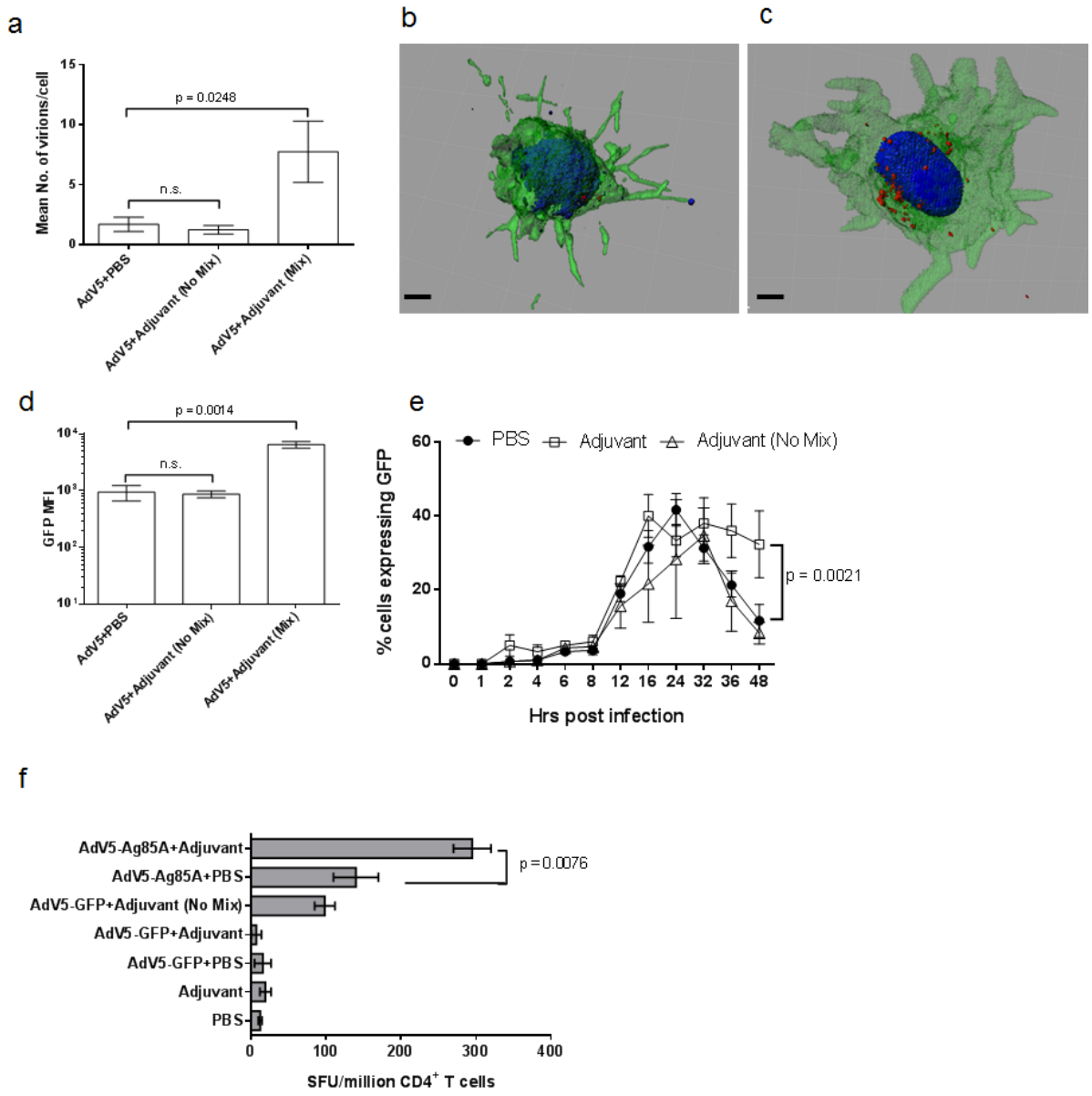
a
Mean No. of virions/cell
p = 0.0248
n.s.
AdV5+PBS
AdV5+Adjuvant (No Mix)
AdV5+Adjuvant (Mix)
b
c
d
GFP MFI
p = 0.0014
n.s.
AdV5+PBS
AdV5+Adjuvant (No Mix)
AdV5+Adjuvant (Mix)
e
PBS
Adjuvant
Adjuvant (No Mix)
% cells expressing GFP
p = 0.0021
Hrs post infection
f
AdV5-Ag85A+Adjuvant
AdV5-Ag85A+PBS
AdV5-GFP+Adjuvant (No Mix)
AdV5-GFP+Adjuvant
AdV5-GFP+PBS
Adjuvant
PBS
p = 0.0076
SFU/million CD4+ T cells

Supplementary Figure 1

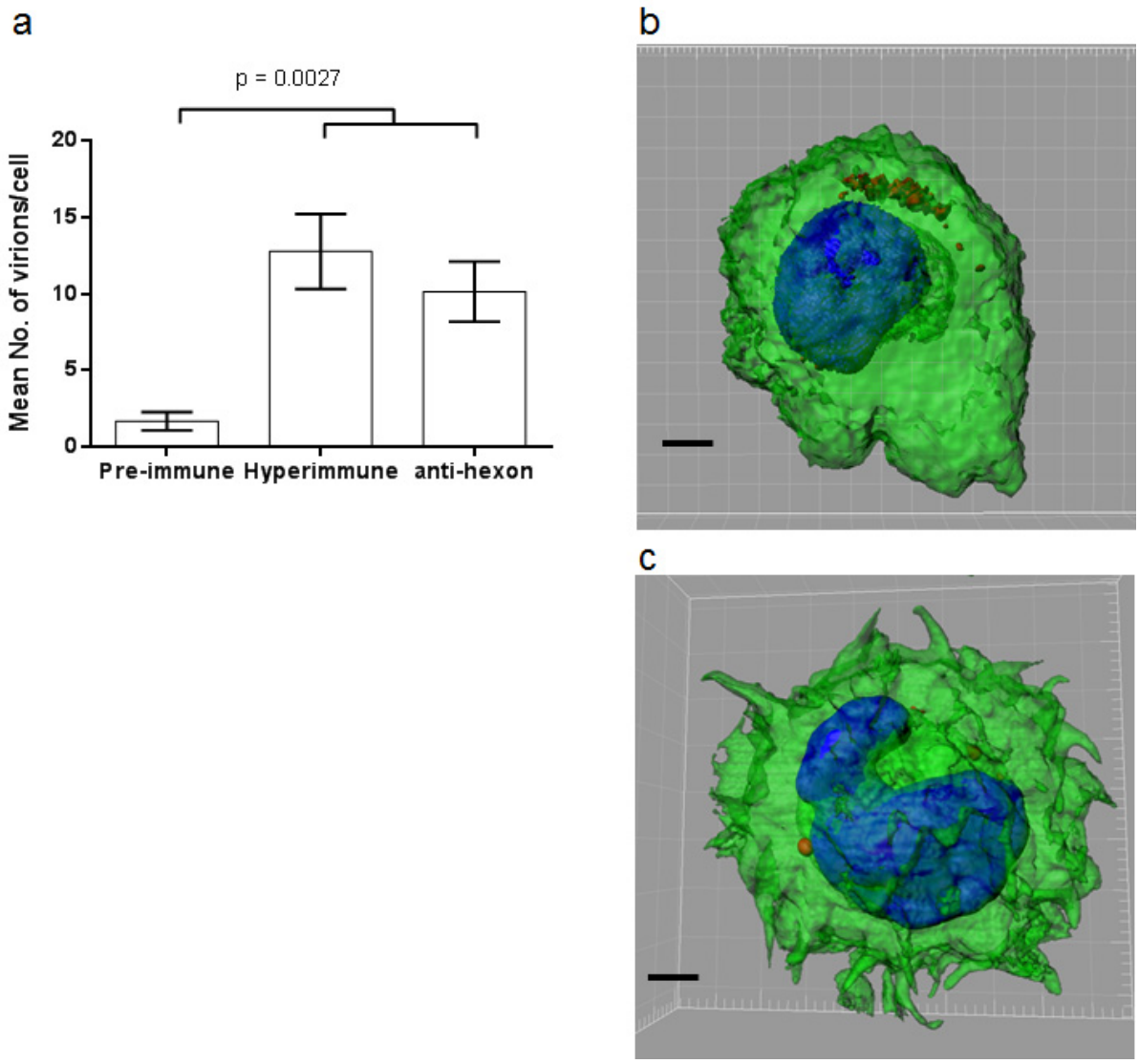

S1. Neutralizing antibodies do not prevent virus entry into ALDC. AF568-labelled AdV5 was mixed with PBS, normal bovine sera or bovine hyperimmune sera to AdV5 and incubated for 60 min after which the mix was added to ALDC as described in Materials and Methods and confocal microscopy was used to quantify the number of intracellular AF568-labelled virions. a) Mean number of intracellular $AF568^{+}$ particles per cell. Bars indicate means of cells from 5 different animals analysed in duplicate and error bars indicate standard error of the means. b and d) Three-dimensional reconstructions from confocal micrographs showing ALDC cultured for 5 hrs with AdV5-AF568 previously incubated with hyperimmune sera (b) or normal sera (c). Reconstructions are representative of cells from 5 independent experiments. Black bar indicates 5 microns.